

UNCLASSIFIED



Australian Government

Department of Defence

Science and Technology

The Mechanical Metallurgy of Armour Steels

S.J. Cimpoeru

Land Division

Defence Science and Technology Group

DST-Group-TR-3305

ABSTRACT

Armour steels have historically delivered optimised ballistic performance against a range of battlefield threats and continue to be highly competitive armour materials. The relationship between armour steel mechanical properties, specifically their mechanical metallurgy, and ballistic performance is explained, where such performance is primarily determined by material strength, hardness and high strain rate behaviour. Other important topics such as toughness; the adiabatic shear phenomenon; structural cracking; and dual hardness and electrosag remelted armour steels are also discussed along with armour steel specifications and standards.

RELEASE LIMITATION

Approved for public release

UNCLASSIFIED

UNCLASSIFIED

Produced by

*Land Division
Defence Science and Technology Group
506 Lorimer Street
Fishermans Bend VIC 3207*

Telephone: 1300 333 362

*© Commonwealth of Australia 2016
October 2016
AR-016-722*

APPROVED FOR PUBLIC RELEASE

UNCLASSIFIED

UNCLASSIFIED

The Mechanical Metallurgy of Armour Steels

Executive Summary

Armour steels have historically delivered optimised ballistic performance against a range of battlefield threats and continue to be highly competitive armour materials. However, the factors that are most important for the ballistic and structural performance of armour steels are not commonly well understood. This report seeks to redress this and provide an overview reference document for armour designers and armoured vehicle capability acquisition and quality assurance engineers.

The relationship between the mechanical properties of armour steels, specifically their mechanical metallurgy, and ballistic performance is explained, where such performance is primarily determined by material strength, hardness and high strain rate behaviour. Other important topics such as toughness; the adiabatic shear phenomenon; structural cracking; and dual hardness and electrosag remelted armour steels are also discussed along with armour steel specifications and standards. It is considered that armour steels will not only continue to improve but will continue to dominate vehicle armour designs well into the future.

UNCLASSIFIED

UNCLASSIFIED

This page is intentionally blank

UNCLASSIFIED

Contents

1. INTRODUCTION.....	1
2. STRENGTH AND BALLISTIC PERFORMANCE	1
3. HARDNESS	3
4. STRENGTH AND HIGH STRAIN RATE EFFECTS	6
5. TOUGHNESS	14
6. ADIABATIC SHEAR.....	18
7. STRUCTURAL CRACKING	21
7.A. Cracking associated with Welding.....	22
7.B. Fatigue Cracking	23
7.C. Stress Corrosion Cracking.....	23
7.D. Delayed Cracking	23
8. SPECIALITY ARMOUR STEELS	24
8.A. Dual Hardness and Maraging Steels.....	24
8.B. ESR Steels.....	27
9. ARMOUR STEEL SPECIFICATIONS AND STANDARDS	28
10. CONCLUSIONS.....	32
11. REFERENCES	32

This page is intentionally blank

1. Introduction

Armour steels have historically delivered optimised ballistic performance against a range of battlefield threats, including both armour piercing and fragmentation threats. Such protection is provided at realistic areal densities for many ballistic applications and also for an affordable price. Steels continue to be highly competitive armour materials and their performance continues to improve with incremental advances in steel metallurgy. The relationship between mechanical properties, specifically the mechanical metallurgy, of armour steels and ballistic performance is the subject of the current study. While the composition, processing and microstructure of an armour steel will determine its mechanical properties which then can be correlated to and will critically determine its penetration resistance, the important influence of such metallurgical factors is not discussed here and the reader is referred elsewhere, for instance, the classical work of Manganello and Abbott [1].

2. Strength and Ballistic Performance

A simple equation can be used to introduce the relationship between the most fundamental mechanical property of an armour, i.e. its strength, and its resistance to penetration by armour piercing projectiles [2,3].

One of the most common and fundamental failure mechanisms experienced by homogenous metal armour, i.e. ductile hole formation, is shown in Figure 1. This failure mechanism exhibits considerable plasticity and hence an estimate of the work performed in plastic deformation should provide a reasonable guide to the kinetic energy required to defeat a target¹. The work of ductile hole formation, W_{DHF} , is equal to the work done in expanding a hole in a target to the projectile diameter [2,3]:

$$W_{DHF} = \frac{\pi D^2 h_0 \sigma_0}{2} \quad (1)$$

where D is the diameter of a non-deforming² projectile, h_0 the target thickness and σ_0 an appropriate compressive flow stress as the measure of material strength. The plastic strains required for the defeat of a metal target are large and hence a compressive flow stress at a high value of strain is appropriate. Estimates of the flow stress at large quasi-static strains are dependent on the actual rate of work hardening [4] and in the present instance, a uniaxial quasi-static compressive flow stress at a true strain of 1.0 is used [3]. At

¹ The failure mechanism with the lowest energy consumption will be the failure mechanism adopted in a particular projectile – target interaction.

² If a projectile deforms, as is the case with ball projectiles, e.g. copper-jacketed lead projectiles, then the work done and ballistic limit is greatly overestimated by Eqn 1 and other predictive methods are better applied.

this level of strain for metals, such a flow stress is usually insensitive to any further increases in strain. High strain rate materials properties at large strains can alternatively be used but may not necessarily offer significantly greater accuracy when making first-order estimates of ballistic performance with Eqn 1 (refer Section 3).

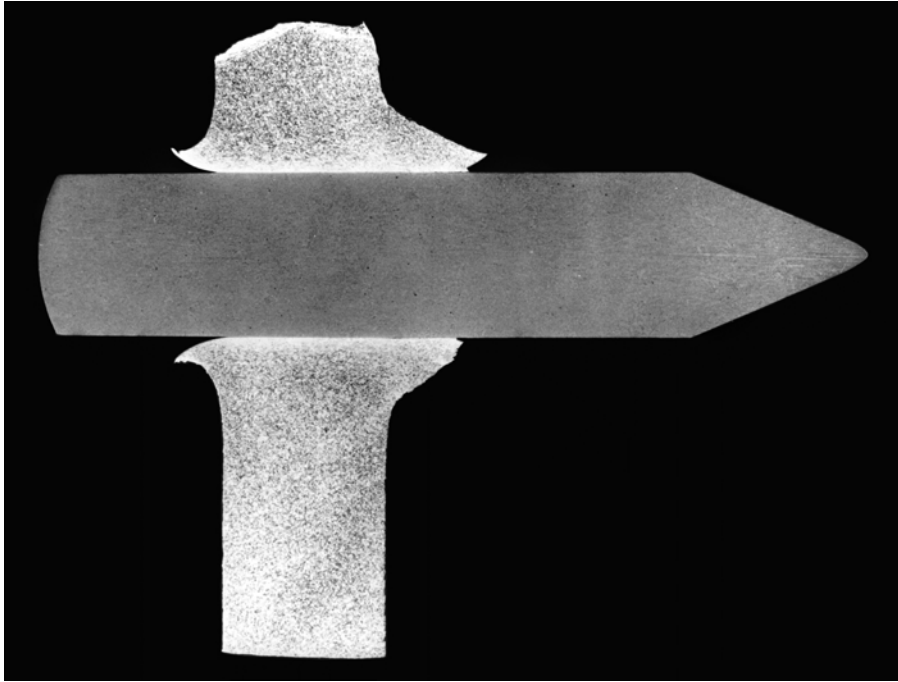


Figure 1: Example of a mild steel plate perforated by a conical, non-deforming projectile, illustrating the ductile hole formation failure mechanism (from [3]).

Using Eqn 1 and equating it to the kinetic energy of the projectile penetrator, where m is its mass, the velocity, v , or ballistic limit of an armour material to protect against that penetrator can be estimated by:

$$v = \sqrt{\frac{\pi D^2}{m} h_o \sigma_o} \quad (2)$$

where $\sqrt{\pi D^2/m}$ is a constant for a given projectile threat condition.

Eqn 2 can be used to estimate the ballistic limits of various homogenous metal targets by non-deforming projectiles and gives reasonable estimates, particularly for targets that experience a ductile hole mechanism of failure [3]. Under-predictions of ballistic limit are usually made because Eqn 2 only accounts for the most significant mechanism of energy consumption, i.e. plastic flow, and second-order terms, such as inertia, friction, nose shape effects, etc., are neglected. The under-prediction of ballistic limit is, however, acceptable as it provides a conservative first-order estimate for protection calculations in all cases where

ductile flow failure occurs [3]. However, caution is appropriate when other failure mechanisms, e.g. adiabatic shear plugging or even brittle failure, might occur [3].

The use of quasi-static yield stress rather than flow stress at high strain values would provide a greater underestimate of the ballistic limit and the discrepancy would be significant for materials that have high rates of work hardening [3]. Hardness measurements should also be used with caution as a measure of material strength as they usually can only be used to estimate the material yield stress³.

3. Hardness

At impact speeds below 2 kms⁻¹, the response of an armour is primarily determined by material strength and toughness and projectile type [5]. Plastic work is therefore the key determinant of the ballistic performance of armour with the penetration resistance of armour steels initially increasing with increasing flow stress. However, a complex relationship exists between the strength of an armour steel plate and its penetration resistance, shown schematically in Figure 2(a) [5] where hardness is used to characterise material strength.

The initial improvements that occur with increases in plate hardness in Figure 2(a) are a result of increased resistance to plastic flow in a ductile hole formation failure mechanism. Beyond a certain point, however, increased plate hardness results in decreased protection due to an increased susceptibility of the material to low-energy adiabatic shear failure (refer Section 6); further increases in plate hardness results in improved performance, but rather as a result of projectile fracture. At very high hardness levels, a lack of toughness can result in brittle fracture of the steel plate and thus erratic behaviour, depending on the specific steel impacted. Figure 2(b) [1] suggests a similar relationship to the schematic of Figure 2(a) but with hardness values specified for the discontinuity in behaviour.

³ The compressive yield stress, σ_y , (in MPa) can be related to Vickers Hardness, H_v , (in kg/mm²) [6] by:

$$\sigma_y = \frac{H_v g}{3}$$

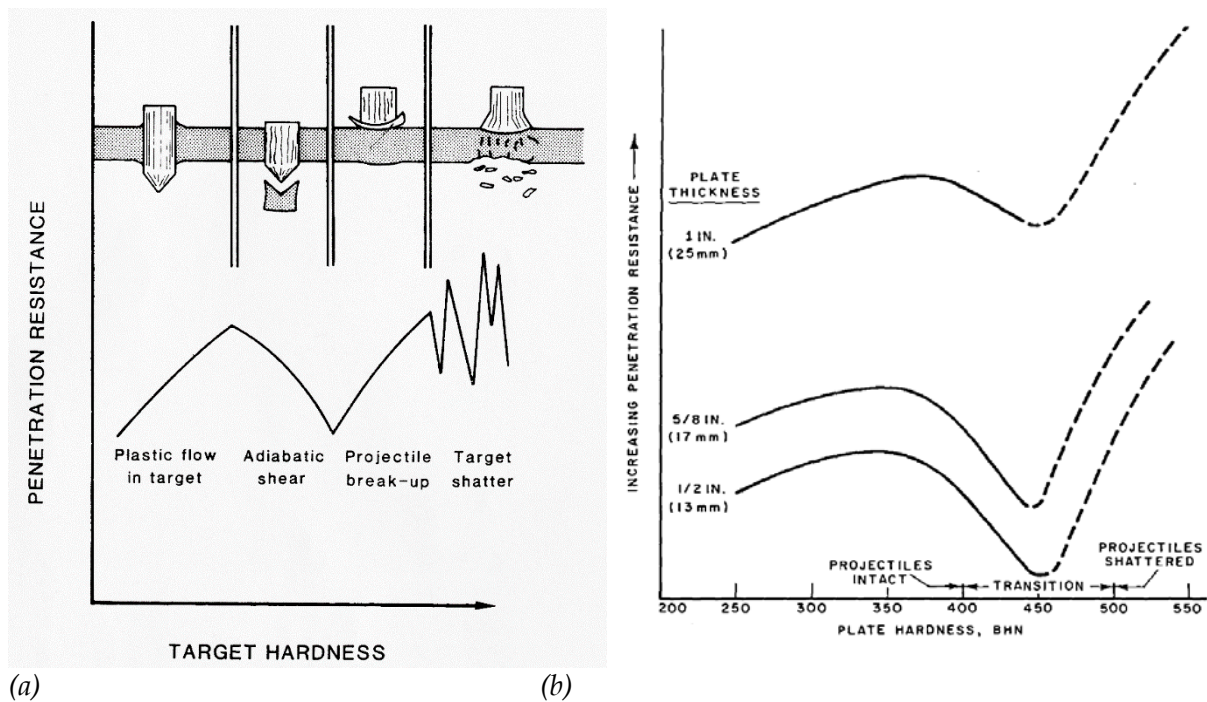


Figure 2: The relationship between the hardness of a monolithic armour steel plate and its performance against armour piercing projectiles. Changes in failure mechanisms result in a complex, discontinuous relationship between plate hardness and penetration resistance, expressed schematically (left, from [5]) and in terms of Brinell hardness values (right, from [1]) for an unspecified armour piercing projectile.

While ballistic performance can sometimes be correlated to a hardness, material hardness is simply a quasi-static measure of yield pressure for a specific indenter geometry that can be related to a compressive yield stress and thus the initiation of quasi-static plastic flow [7]. Hardness is not a measure of a dynamic yield or flow stress that accounts for work hardening, strain rate hardening or thermal softening (refer Section 4) as would be required to fully define the armour material resistance to plastic flow under projectile impact conditions.

Figure 3 shows how the ballistic limit varies for a wide range of practical armour steel hardness values [8,9] from rolled homogenous armour (RHA) [10] through high hardness armour (HHA) [11] to ultra-high hardness armour (UHHA) [12]. The improved ballistic resistance of steel as a function of increasing hardness is well established in the ballistic community, particularly by Rapacki et al. [13] and for this reason armour designers are more often incorporating higher hardness (higher strength) armour steels in their applique and structural armour solutions.

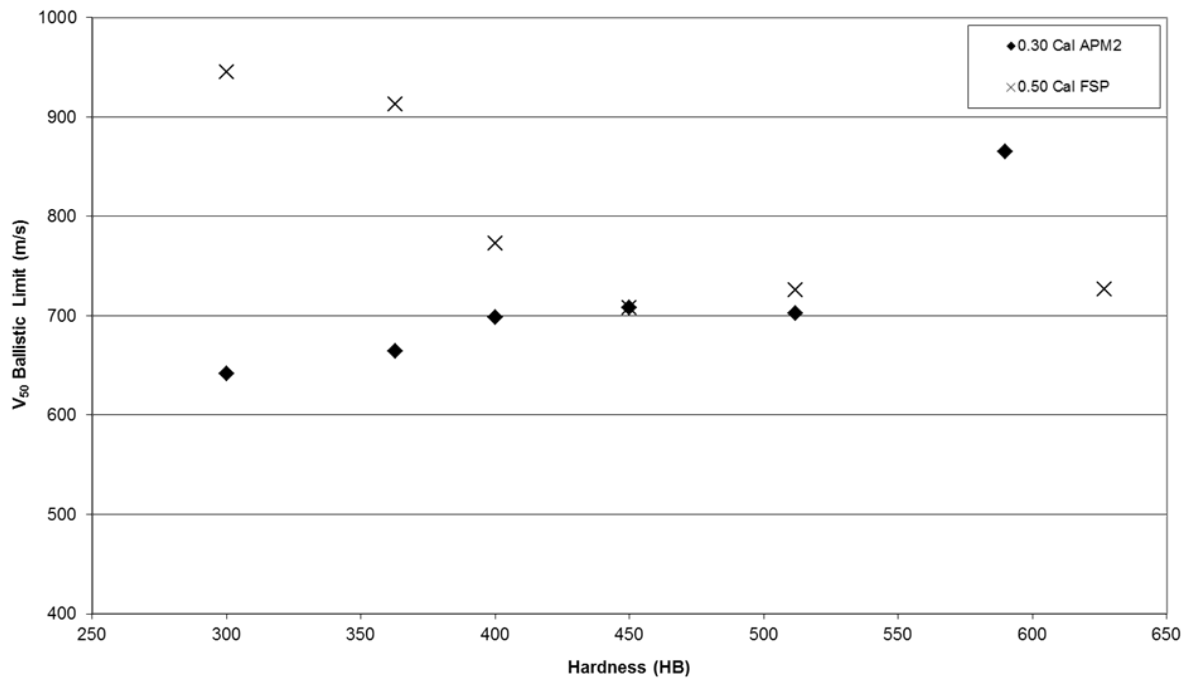


Figure 3: Influence of increase in hardness on the V_{50} ballistic limit for 10 mm Bisalloy armour steel plates against 0.30 Cal APM2 and 0.50 Cal FSPs (after [8,9]).

Whilst increases in hardness increases resistance to projectile penetration (improved protection), this is not always linear and does not necessarily apply for fragmentation protection, as demonstrated by the Fragment Simulating Projectile (FSP) ballistic limits in Figure 3. Fragmentation protection decreases sharply with hardness, making the higher hardness armour grades such as HHA [11] a poor choice for such applications. This reduced penetration resistance arises because impacts of blunt fragments cause high strength steels to fail by adiabatic shear plugging, a low energy failure mechanism [14]. Adiabatic shear is responsible for the observed reduction in FSP performance and plateau in armour piercing projectile penetration resistance between 450-512HB in Figure 3.

As such there is no difference between the ballistic performance of Ultra High Toughness Armour (UHTA) (450HB) and HHA (512HB) which is also seen across other plate thicknesses [8]. The UHTA grade has a leaner alloying element content, providing improved toughness and weldability compared to HHA. UHTA would be a better choice than HHA for structural applications and its more consistent ballistic performance may allow a weight saving for some protection levels [8].

More recently, circa 2008, ultra-high hardness armour UHHA (>570HB) steels have been produced that have been assessed and applied as practical armour materials [15,16]. Figure 4 shows how UHHA steels can offer considerable performance improvements over HHA (also seen in Figure 3) and also fulfil an equivalent ballistic role to dual hardness armour [17] but as a homogenous plate. Ballistic performance increases at very high steel hardness values have been known for many years but it is only recently that armour steels

have been produced that consistently meet ballistic requirements without shattering upon impact (refer Section 5).

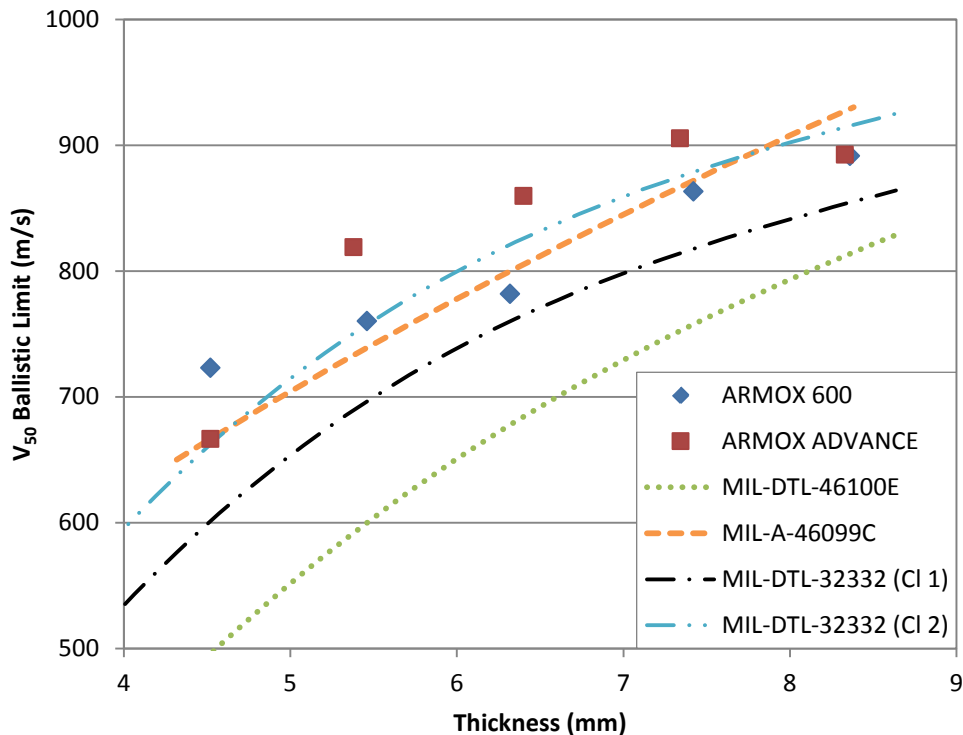


Figure 4: The V_{50} ballistic limit for ARMOX 600 and ARMOX Advance UHHA grades, HHA (MIL-DTL-46100E), dual hardness armour (MIL-A-46099C) and UHHA Class 1 and Class 2 (MIL-DTL-32332) against 0.30 Cal APM2 at 30° obliquity (after [11,12,16,17]).

Overall, Figures 2 and 3 demonstrate that ballistic performance relates to steel armour hardness, though over specific hardness ranges there can be an increasing or decreasing relationship between ballistic performance and hardness, depending on the projectile and the observed armour failure mechanism. Another important influence of armour hardness is whether it is sufficiently high to deform or shatter a projectile, both of which will strongly affect ballistic performance. In practical terms hardness is a measurement of strength that can be easily measured on a plate-by-plate basis, and it is particularly convenient as a quality assurance measurement.

4. Strength and High Strain Rate Effects

Extensive historical studies found that the ballistic performance of structural and armour-grade steels correlates to hardness and tensile strength but not yield strength [1]. Interestingly, Borvik et al. [18] in Figure 5 shows a quite linear relationship with measured quasi-static tensile yield stress between values of 600 and 1700 MPa for quenched and tempered steels.

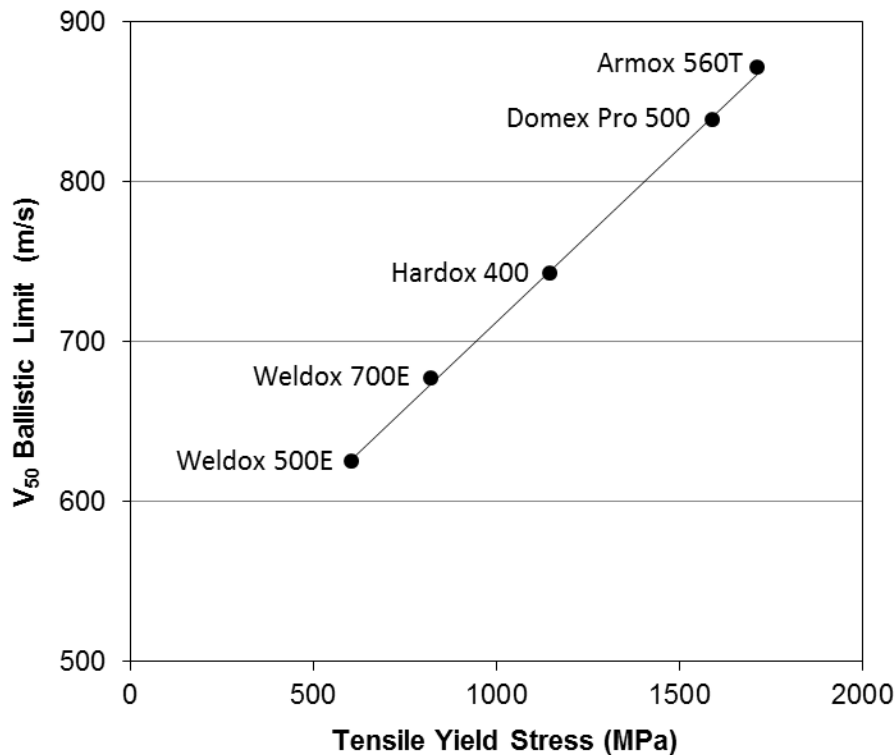


Figure 5: Linear relationship between quasi-static tensile yield stress and ballistic limit for a range of quenched and tempered steels (from [18]).

Woodward [3], however, demonstrated a strong correlation between predicted and measured ballistic performance for a range of materials when the quasi-static compressive flow stress at high strains, i.e. flow stress at a true strain of 1.0, σ_o , rather than compressive yield stress, σ_y , was used as a measure of material strength. The use of flow stress is reasonable when considering the large strains involved in a ballistic impact event, especially through ductile hole formation and many other failure mechanisms. The quasi-static compressive true stress – true strain curve is almost flat at such large strains, Figure 6, thus this flow stress measure is also largely insensitive to the precise value of strain.

Figure 7 shows the experimental vs predicted ballistic limits from ductile hole formation theory, Eqn 2, for two quasi-static measures of material strength, i.e. σ_o and σ_y , for two different projectile and five different material conditions for targets that fail by a ductile hole formation mechanism. A line depicting a 1:1 relationship between experimental and predicted ballistic limits also demonstrates that conservative under-predictions of the data points are obtained using ductile hole formation theory⁴. The use of a flow stress based on σ_o is shown to provide more accurate predictions of the ballistic limit [3].

⁴ The data point that is an exception relates to Hadfields manganese steel that has abnormally high work hardening ($n = 0.4$) and is excluded from this analysis as the key assumption that the flow stress is insensitive to the precise value of strain at large strains no longer applies.

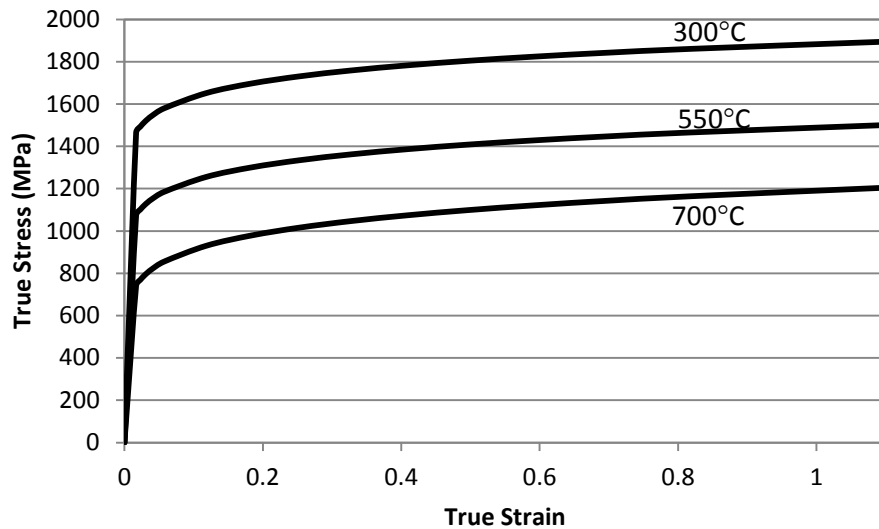


Figure 6: Compressive quasi-static true stress - strain curves for a 4130 steel that has been quenched and tempered at 300 °C (480HV), 550 °C (370HV) and 700 °C (260HV) with flow stresses described by $\sigma = \sigma_0 \varepsilon^n$ [19].

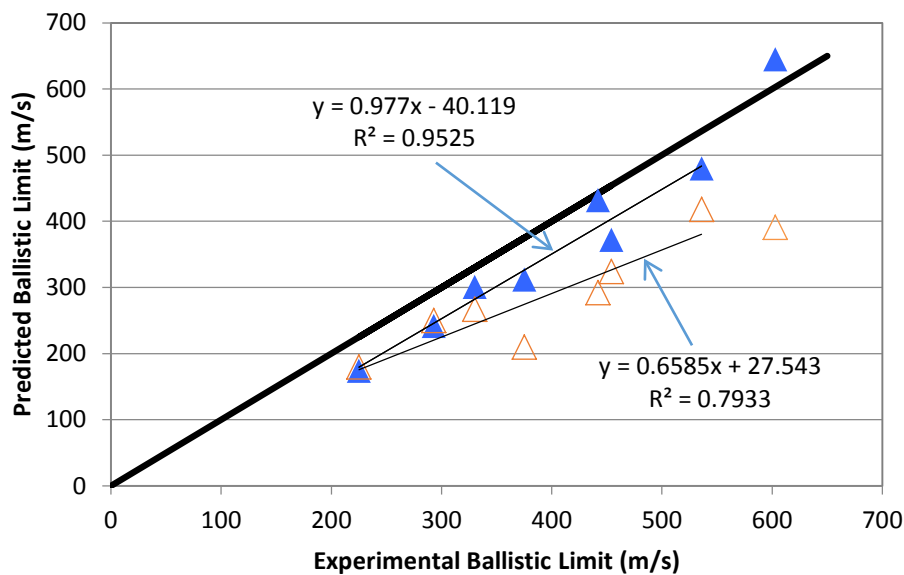


Figure 7: Experimental vs predicted ballistic limits from ductile hole formation theory, Eqn 1, for two quasi-static measures of true compressive strength, σ_0 (closed symbols) and σ_y (open symbols) [3]. Linear regression lines are plotted through all data except for the data point with abnormally high work hardening.

High rate uniaxial compression testing is most often used to measure dynamic material properties as it allows the large strains of ballistic impact to be achieved at the highest strain rates. The effect of strain rate on the stress-strain performance of mild steel [20,21] and representative armour steels [22] is shown in Figures 8 and 9. The observed increase in

flow stress with strain rate is known as strain rate hardening or a strain rate effect. Dynamic loading is shown to considerably enhance the flow stress of steels in the vicinity of the yield and initial flow stresses.

Figures 8 and 9 show that at high loading rates the flow stress at large plastic strains appears unaffected by the loading rate with the initial flow stress tending to approach the value of the quasi-static flow stress at large plastic strains. Strain rate hardening is occurring, but the overall shape of the stress-strain curve is modified as a result of thermal softening due to adiabatic heating associated with the large, high rate plastic deformations. In other words, the flow curve is a combination of a flow stress increase due to strain rate hardening as well as a decrease due to thermal softening, which together can lead to flattened stress-strain curves at high loading rates as seen in Figures 8 and 9.

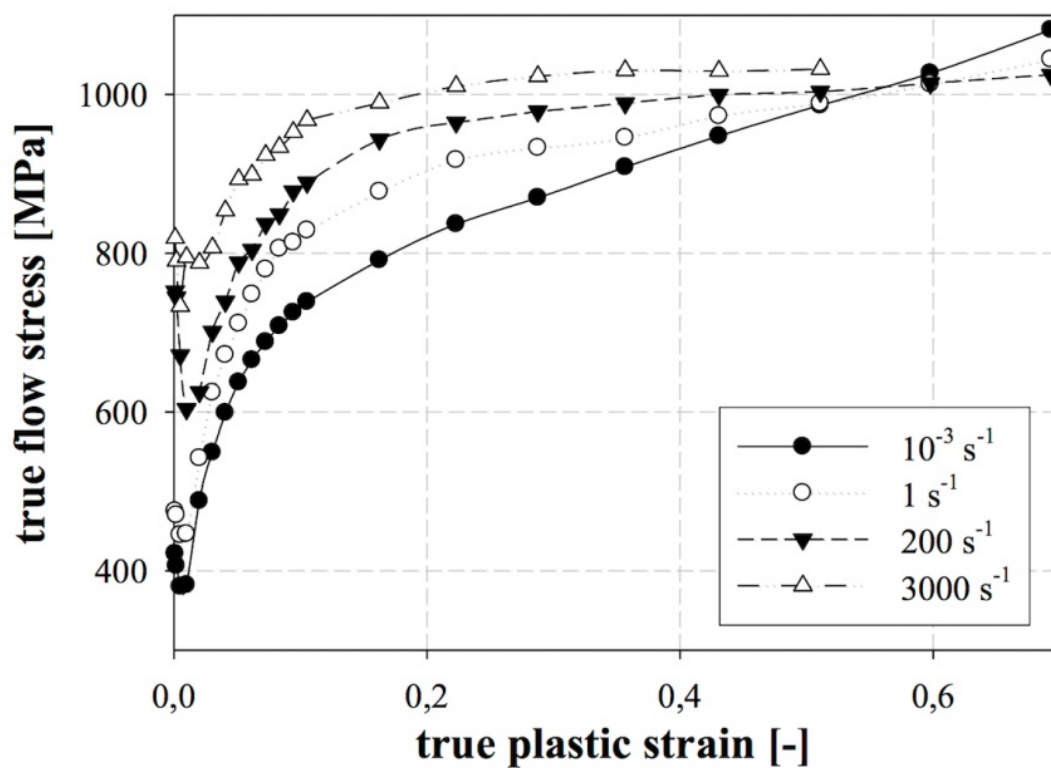


Figure 8: Compressive true stress - strain curves for a 1045 steel (from [21]).

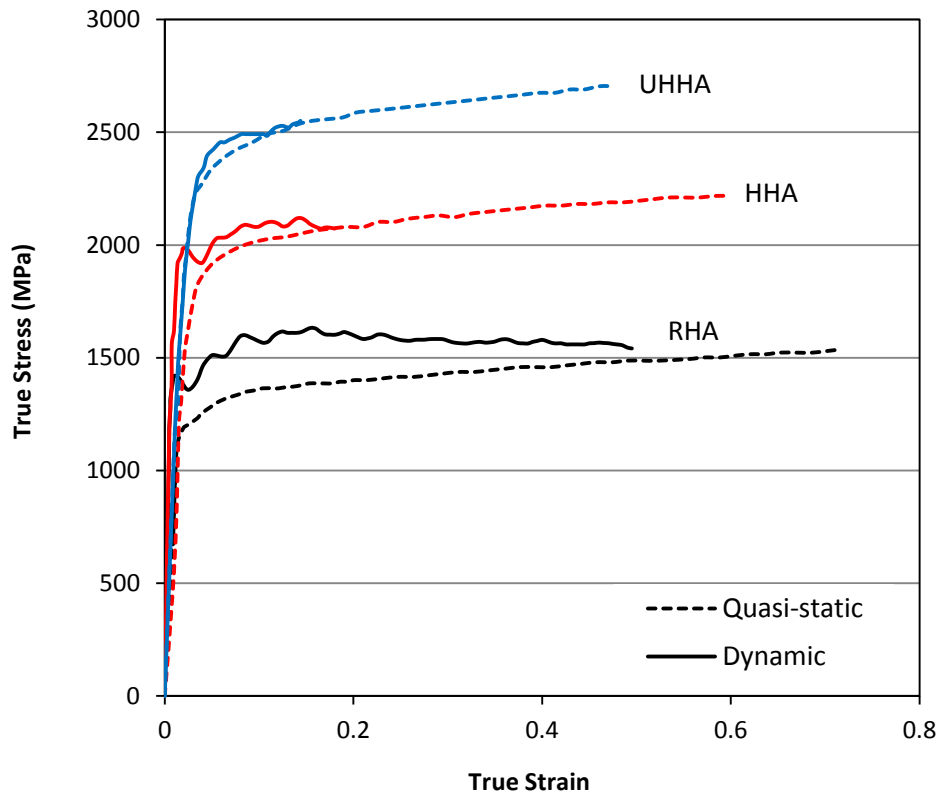


Figure 9: Compressive true stress – strain curves for MARS armour steels, MARS 190 (RHA), MARS240 (HHA) and MARS300 (UHHA) with dynamic strain rates of $4800s^{-1}$, $3800s^{-1}$ and $1500-2500s^{-1}$, respectively (from [22]).

Considering the loading rates relevant for ballistic impact and the effect of loading rate on the stress-strain performance of steels, refer Figures 8 and 9, an assumption of rigid-plastic stress-strain behaviour based on a quasi-static compressive flow stress at a large strain can be a reasonable approximation for the material behaviour in some instances, e.g. for use in one-dimensional analytical models [3]. However, high strain rate testing is normally used to provide greater fidelity and understanding of material behaviour, including its failure behaviour, and is used to populate material models employed for numerical modelling.

What is the reason for the enhancement in the flow stress of steel at high strain rates? In the vicinity of the initial flow stress, flow stress is affected by both temperature and strain rate, and strain rate enhancement can be explained by the Thermal Activation Model of dislocation movement. This model assumes that at temperatures lower than a critical temperature (dependent on strain rate), the flow stress depends on both an athermal component and a thermally activated component [23]. The athermal component of flow stress is determined by the effect of long range dislocation obstacles (e.g. grain boundaries, precipitates, etc.) and is largely strain rate independent, but still dependent on temperature. The thermally activated component of flow stress is related to short-range obstacles (e.g. dislocations) which can be overcome by thermally activated glide of mobile slip dislocations due to thermal fluctuations and thus is more strongly affected by temperature and strain rate; and it is increased by either decreasing temperature or

increasing strain rate [23]. Decreasing temperature leads to reduced thermal energy while increasing strain rate reduces the time available for dislocation movement. Both circumstances result in a reduced ability of mobile dislocations to overcome short range obstacles and hence lead to strain rate hardening.

Figure 10 shows that the Thermal Activation Model [23] successfully describes stress-strain behaviour at initial flow stresses from low to very high strain rates, i.e. from strain rates of 10^{-3} to 10^5 s^{-1} . Other models do not effectively account for the observed behaviour [21].

However, the Thermal Activation Model was originally established for initial flow stresses. While this model can also be applied to larger strains, this is seldom done as there are no closed form solutions available that describe the stress-strain behaviour as a function of plastic strain, strain rate and temperature. At larger strains, empirical models such as those of Johnson-Cook [24] or the semi-empirical model of Zerilli-Armstrong [25] are often used to describe flow stress behaviour as a function of strain, strain rate and temperature.

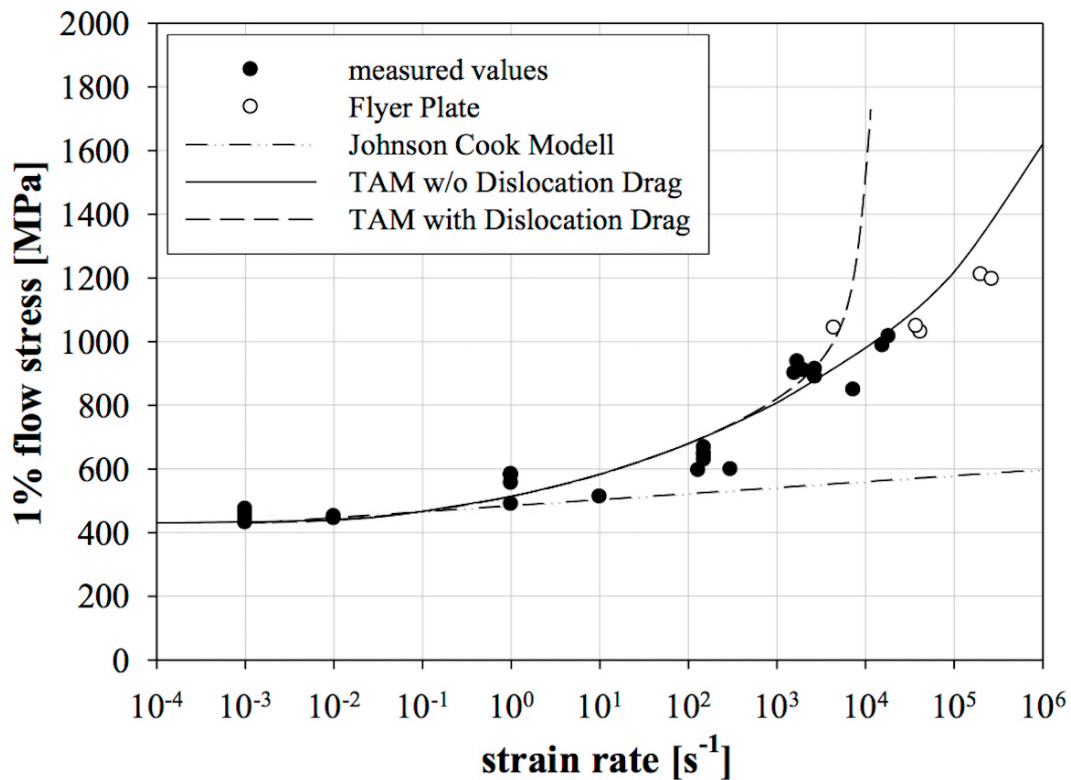


Figure 10: Compressive true flow stress at 1% true plastic strain for 1045 steel at strain rates from 10^{-3} to 10^5 s^{-1} , compared to the Thermal Activation Model (TAM), TAM with Dislocation Drag and the Johnson Cook Model (from [21]).

Dynamic tensile properties have also been measured. Figure 11 compares quasi-static tensile and dynamic tensile properties for a range of quenched and tempered steels.

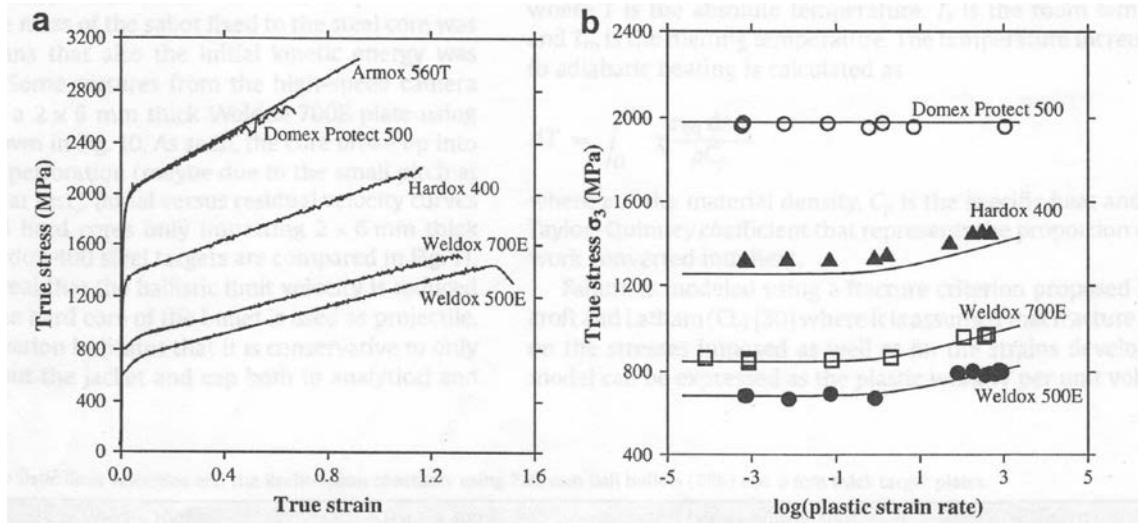


Figure 11: Tensile quasi-static true stress - strain, (a), and true stress - strain rate curves for a range of quenched and tempered steels (from [18]).

The difference between quasi-static compressive and tensile properties of quenched and tempered steels is the Strength Differential [26]. This also applies under dynamic loading [27]. The Strength Differential arises because of different material responses between compressive and tensile loading due to a number of potential metallurgical reasons such as: the presence of microscopic cracks and quench cracks arising from hardening; dislocation movement against grain boundaries or inclusions; texture effects and anisotropy arising from prior plastic deformation. Also, under tensile loading, micro-cracks propagate, thus increasing material volume and thus greater plastic strains. Under compressive loading, micro-cracks are forced closed, resulting in lower measured plastic strains. Any retained austenite phase left over after quenching and tempering processes will also have different behaviour under tension compared to compression [27]. Figure 12 shows that the differences in stress - strain behaviour between compression and tension can be quite significant for quenched and tempered steels and demonstrates the ability of the Johnson-Cook [24] and Zerilli-Armstrong [25] models to represent the material behaviour at representative strain rates.

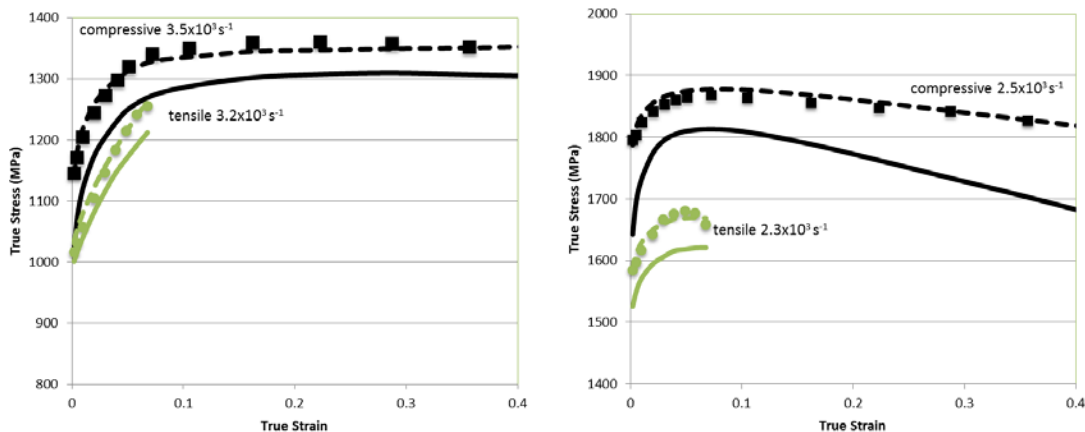


Figure 12: Compressive and tensile flow stresses for two quenched and tempered steels at nominal identical strain rates: left, 290HV30 (tensile $3.2 \times 10^3 \text{ s}^{-1}$ and compressive $3.5 \times 10^3 \text{ s}^{-1}$) and right, 410HV30 (tensile $2.3 \times 10^3 \text{ s}^{-1}$ and compressive $2.5 \times 10^3 \text{ s}^{-1}$) (after [27]). Associated Zerilli-Armstrong, -----, and Johnson-Cook, ———, predictions are also shown.

Armour steels are available in a range of thicknesses, and as a consequence material properties vary due to the difficulty in achieving sufficient quench rates during heat treatment to achieve consistent and high hardness through-out thicker plates. This is observed for RHA which is available in a wide range of thicknesses (2.5 to 150 mm). The thicker armour sections are produced with higher alloying content to increase their hardenability but changes in composition cannot always fully compensate for such significant changes in thickness, resulting in reduced hardnesses in the middle of the cross-section for thicker plates. Figure 13 clearly shows how the dynamic properties of RHA are affected by hardness, a consequence of plate thickness, where thicker plates also have lower surface hardnesses [28]. Note the tendency for these steels to effectively exhibit rigid-plastic behaviour with increasing strain rate, due to a combination of strain rate enhancement at the initial flow stresses and a flattened stress-strain due to thermal softening at larger plastic strains.

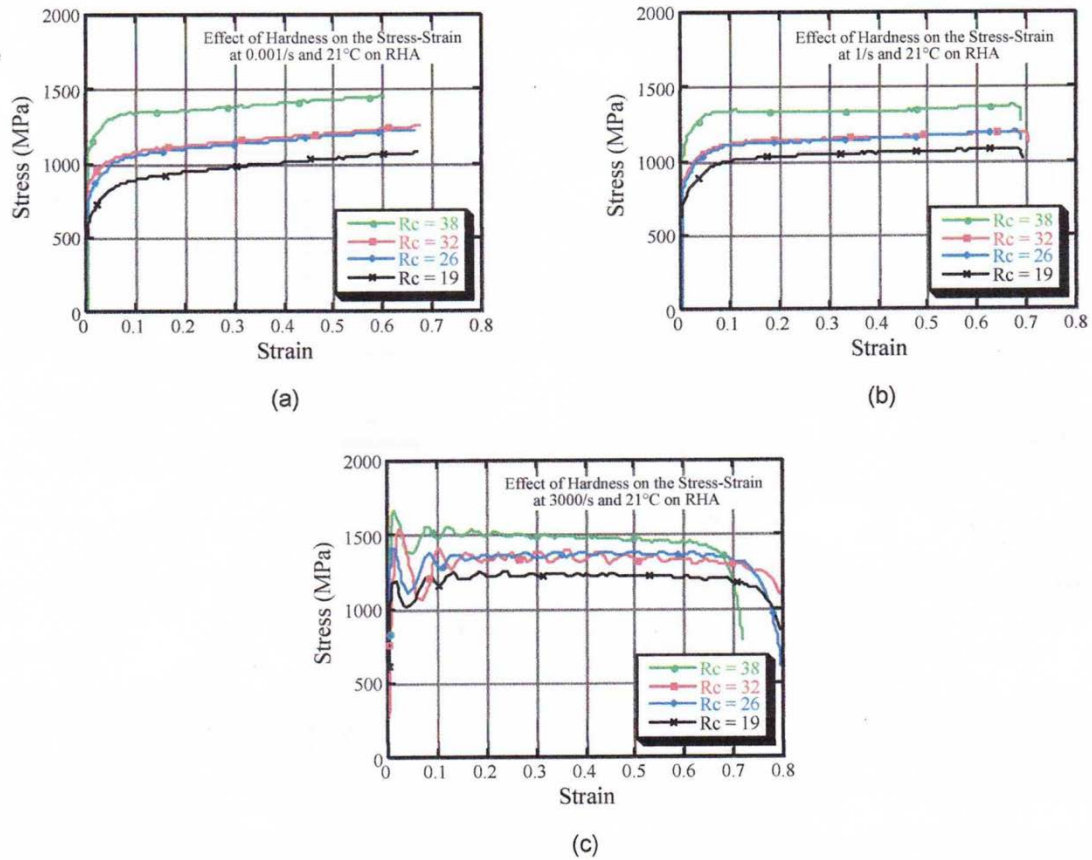


Figure 13: Compressive stress – strain curves at different surface hardnesses ($HRc\ 38 \cong 353HB$, $HRc\ 32 \cong 301HB$, $HRc\ 26 \cong 258HB$ and $HRc\ 19 \cong 223HB$) for RHA at strain rates of: (a) $0.001\ s^{-1}$; (b) $1\ s^{-1}$; and (c) $3000\ s^{-1}$. (from [28]).

5. Toughness

Shattering of armour plate upon ballistic impact can be described as occurring when the ductility of an armour plate is insufficient to withstand the strains associated with bending arising from an impact and bending is the preferred failure mechanism [29]. It is found when a plate fractures with little discernible deformation and can also be combined with other failure mechanisms, Figure 14. Armour plate shattering is a catastrophic event.

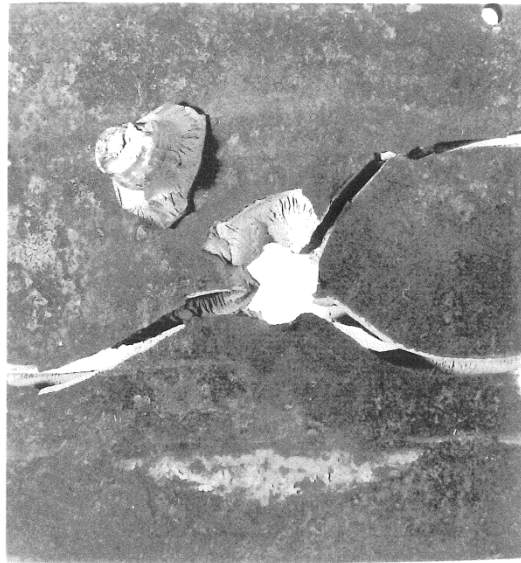


Figure 14: Armour steel failure by a combination of shattering and discing. Note that the disc is associated with a partially-formed plug (from [29]).

In a uniaxial tensile test ductility is measured by the fracture strain which accounts for both homogenous strain and the necking strain after the ultimate tensile strength has been reached. For a ductile material, ductility is a uniaxial measure of the total elastic and plastic strain before micro-void formation, growth and coalescence leads to final fracture. The shattering failure mechanism is of course an example of brittle fracture. Such fractures typically involve rapid crack propagation, exhibit little plastic deformation and can even occur in steels that exhibit ductile behaviour!

In practical terms, the utility of a material for demanding applications such as resisting ballistic or blast loading depends on how it responds in the presence of notches or cracks. Notches will produce high local stresses and a high local magnification of the strain rate at the root of a notch [30]. Importantly, notches will also lead to a three dimensional multiaxial stress state that is particularly severe directly in front of a notch and even more so in front of a crack.

Here the ability for local dislocation glide controls the ductility, defined as "toughness" in these circumstances. Toughness is always related to and specific to the three dimensional stress field which prevents or hinders global plastic flow, i.e. dislocation movement. Yielding, and thus plastic flow, takes place in only a small volume of material because it is only locally at the root of the notch or at the crack tip where the local stress exceeds the yield stress.

High strength materials, including some armour steels (where the ductility, even in a uniaxial case, is often very low), often have small local plastic zones (and thus very high local stresses) in front of cracks [30]. Even with low external forces, a high local stress can be produced which can result in rapid micro-crack propagation and fracture. Steels with high work hardening and high fracture strains are preferred as they can produce a large

plastic zone in front of any incipient cracks which can provide greater resistance to crack propagation. The advantage of such steels is that the larger plastic zone at the root of a notch or crack extends the elastic loaded region into an area where the stresses will be much, much less. Hence such steels have much greater resistance to fracture.

Armour steels have orthotropic mechanical properties, particularly toughness, which is much greater in the plate longitudinal and transverse directions compared to the short transverse (through thickness) direction. This is caused by the segregation of alloying elements, particularly sulphur based non-metallic inclusions, during the casting process, as well as the orthotropic deformation of the microstructure during the rolling process. All of this leads to microstructural banding in steels. Leach and Woodward [31] showed that the ballistic resistance and failure mechanism of a quenched and tempered steel varied as a function of the orientation of the microstructural banding in the plate.

Toughness also becomes an important issue for thick armour plates due to the triaxial stress state caused by the higher constraint of the thicker sections [1]. In such circumstances, the stress state due to a notch approaches plane strain rather than plane stress, the former state having a lesser stress for fracture [31]. Thicker armour steels will in general need to have higher alloy content to increase their toughness to better manage triaxial stress states [1].

Mackenzie et al. [32] showed that fracture strain is sensitive to stress state (i.e. degree of triaxiality) in a range of high strength steels and, as would be expected, there were significant differences between in-plane and through-thickness fracture strains. Sato et al. [33] showed that there was not a significant influence of strain rate on the fracture strain for a range of steels above 600 MPa tensile strength, at least for strain rates up to 10^2 s^{-1} , but failure is complex and it is difficult to state general conclusions. Other factors such as temperature and the rate of loading or strain rate can also strongly reduce toughness [30]. Whittington et al [34], for instance, examined the ductile fracture morphology of an RHA armour steel and found that an increase in strain rate resulted in smaller ductile void formation. Conversely, an increase in test temperature resulted in larger ductile void formation and thus greater failure strains.

Charpy impact testing is used to assess whether steels meet certain minimum levels of toughness (measured in Joules for fracture) for different armour applications [35]. Testing is conducted at -40°C as this temperature is usually sufficient to enable brittle behaviour to be distinguished and allows a relative measure of toughness under such circumstances. The Charpy test can help distinguish low and high toughness steels on a comparative basis and hence helps define what armour applications they are best suited for. Ductile (high toughness) or brittle (low toughness) behaviour is determined by examining the fracture surfaces of Charpy specimens that have been tested to failure. For instance, Figure 15 shows scanning electron micrographs of the fracture surfaces of a quenched and tempered steel at two different Charpy impact test temperatures. Figure 15 shows, left, 95% brittle behaviour at -40°C (18J measured) with a cleavage-like, flat fracture surface and, right, 54% ductile behaviour at ambient temperature (84J measured) with a ductile-dimpled fracture surface around the outer portion of the specimen.

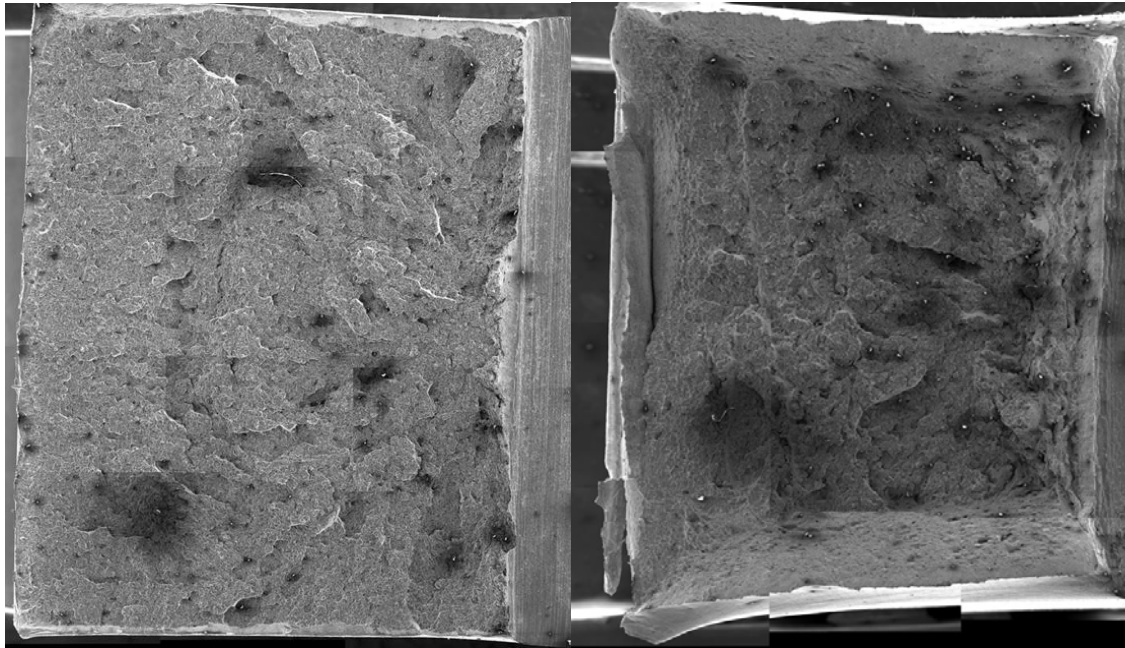


Figure 15: Scanning electron micrographs of Charpy impact specimen fracture surfaces for a quenched and tempered steel at two different test temperatures, showing (left) 95% brittle behaviour at -40°C with a cleavage-like, flat fracture surface and (right) 54% ductile behaviour at ambient temperature with a ductile-dimpled fracture surface and presence of shear lips (ductile material distortion) around the outer portion of the specimen. Crack growth was from the right to left and the samples were taken in the T-L (transverse-longitudinal) direction [36].

Charpy impact testing can be used to measure the ductile to brittle transition temperature which is the temperature at which the material fracture mode changes from one of ductile to brittle behaviour in the Charpy impact test [30]. Low test temperatures impede dislocation movement and thus encourage brittle behaviour [30]. However, ductile to brittle transition temperatures are unique to specific test configurations, stress states and loading rates and thus results from laboratory Charpy tests cannot be used to make definitive predictions of the behaviour of real armoured structures at field temperatures.

While the Charpy test is an important and practical means to assess and rank the toughness of different armour steels, fundamentally it is an empirical test with an ill-defined triaxial condition at the notch and this is why it cannot be used to predict the onset of brittle fracture [30]. Impacts or blasts produce very high local stresses which can easily initiate cracks. Whether or not such cracks propagate and lead to brittle fracture relates to material-specific crack propagation properties that are not measured by the Charpy test [37]. Herzig et al. [37] conducted Charpy tests as well as blast tests that measured crack propagation for a range of steels and have shown that the rankings from such tests vary with test temperature (-40°C versus ambient temperature). Importantly it was shown that there was a good correlation between material toughness properties and their resistance to crack propagation under high rate (explosive) loading.

Armour toughness has been increased from the relatively alloy lean steel compositions that were designed for low cost volume production in WWII when there were also shortages of critical alloying elements. Higher nickel contents, for instance, have increased toughness and reduced the likelihood of shattering at higher hardnesses, also providing more consistent ballistic perforations and thus tighter ballistic limits. While this increases armour cost and can reduce weldability, increased toughness, particularly in high and ultra-high hardness grades, has been a significant theme in armour steel development over the last 15 years and this trend is expected to continue.

6. Adiabatic Shear

Heat, generated from the work of plastic deformation during impact is usually contained within the deforming material as there is often not enough time for the heat to escape to the surrounding material. These conditions are considered adiabatic for practical purposes, and under such conditions the rate of material softening, due to the temperature rise, can be greater than the rate of work hardening. This can lead to an instability within the microstructure of the material, and a subsequent, sometimes significant, fall-off in material strength. This has important implications for a number of armour materials, particularly high strength steels, where increases in static material strength properties are sometimes accompanied by a reduction in penetration resistance over certain hardness ranges [1,38], Figure 16. This is because of the phenomenon of adiabatic shear [39].

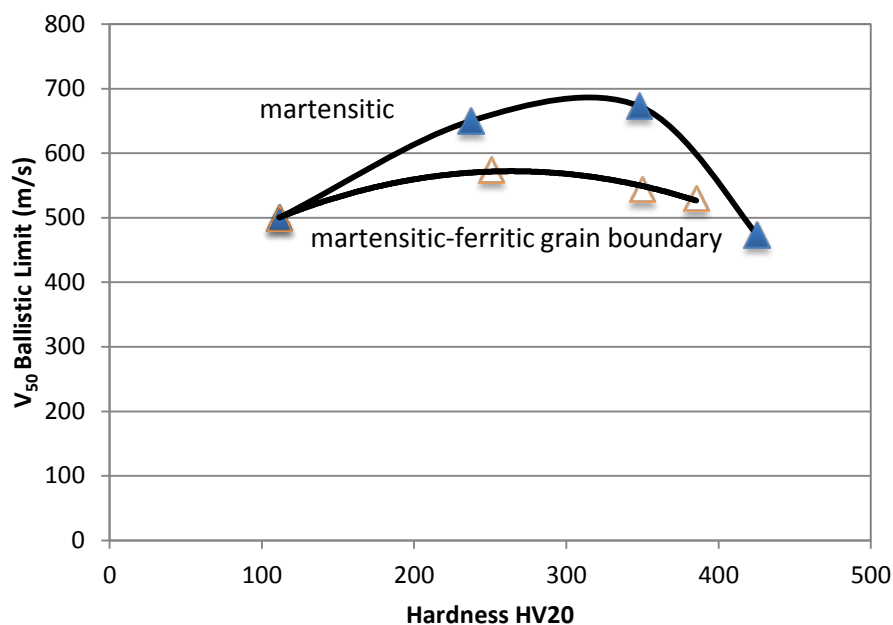


Figure 16: Relationship between ballistic limit and hardness for quenched and tempered steels with a martensitic microstructure, A, and martensitic-grain boundary ferrite microstructure, B (from [38]).

Under a particular set of conditions, there is a significant fall in the material shear yield stress, and the formation and low energy ejection of a plug of armour and thus reduced ballistic resistance as seen in Figure 16 (also shown in Figure 2 where a fall-off in ballistic resistance against fragments is associated with an adiabatic shear plugging failure mechanism). In general, the fall-off in ballistic resistance is expected at about 350HV (~330HB) [38,40], but this will also be affected by the obliquity of the impact [29].

The general theory of adiabatic shear was developed by Zener and Hollomon [39]. Recht [41] further refined the theory to allow a relative ranking of materials in terms of their susceptibility to adiabatic shear by determining a critical shear strain rate from their thermo-mechanical material properties. Low values of specific heat, thermal conductivity, density and work hardening rate were favourable to adiabatic shear along with high values of shear yield stress and the rate of thermal softening.

Once adiabatic shear initiates, the associated fall-off in shear yield stress will cause deformation to concentrate, resulting in bands of intense shear deformation that can be detected in metallographic specimens as they resist etching and appear as a narrow, white-etching band (refer Figure 17) that contrasts with the rest of the more-readily etched steel microstructure. These bands, referred to as adiabatic shear bands, are distinguished by a very fine grain size, very high hardness and exhibit anomalous tempering characteristics [42].

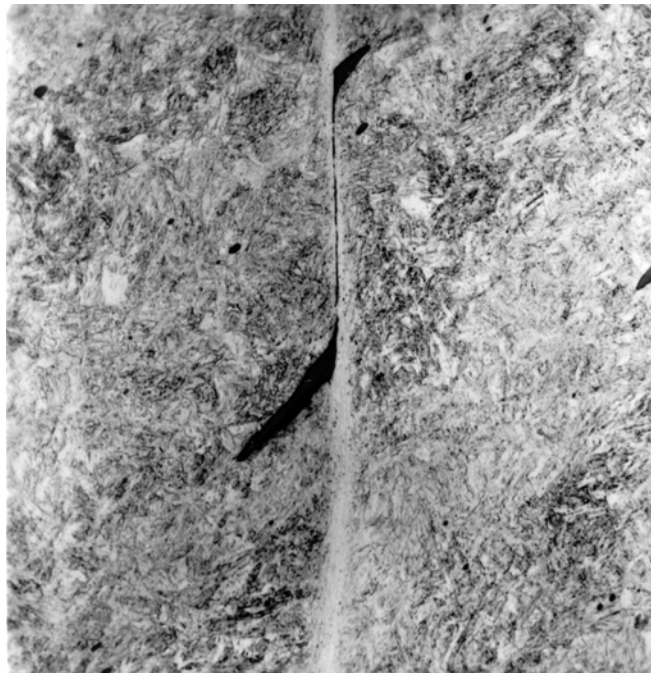


Figure 17: Adiabatic shear band (central white band from top to bottom of image). Significant shear strains are evident from the displacement of the dark inclusion by the shear band (from [14]).

Material susceptibility to adiabatic shear alone does not necessarily result in adiabatic shear failure. Adiabatic shear failure is associated with narrow bands of intense shear

strain, where the shears are of a much greater magnitude than the material would sustain in conventional ductile shear failure. Ductile shear failure involves the exhaustion of ductility through a failure mechanism involving void nucleation, growth and coalescence and thus by comparison greater plastic deformation and work [14,43]. An adiabatic shear failure mechanism occurs when adiabatic shear bands have fully propagated through the thickness of a plate and hence material separation results. This failure mechanism absorbs much less energy than an equivalent ductile shear failure.

The conditions for adiabatic shear failure to occur are complex and not just related to material properties. The likelihood of adiabatic shear failure will also depend on the geometry of the penetrator, being more likely to occur in less susceptible materials when they are impacted by blunt projectiles. Such projectiles tend to produce plugging failures, even when adiabatic shear is not involved.

Reduced strain rate dependent behaviour is known to encourage adiabatic shear failure [44,45]. The simple target geometry of a cylindrical specimen in a high strain rate - compression test allows some of the key requirements for adiabatic shear failure to be identified. In such circumstances, the following conditions are required for adiabatic shear failure:

- a) A negative slope on a material stress-strain curve
- b) A suitable specimen geometry so that intense shear can develop [46]
- c) Conditions, such as friction, that ensure that material deformation/flow can continue in a stable manner over time [47].

On occasion adiabatic shear bands might only develop within a material whereas other shear bands will also intersect free surfaces, allowing material separation and thus adiabatic shear failure to occur. These observations are consistent with the changing direction of material flow over time in many circumstances [43]. Adiabatic shear bands have been correlated with slip lines associated with plastic deformation and in particular in those slip lines that are also velocity discontinuities [48]. Flockhart et al [43] numerically modelled a range of impact problems to demonstrate a correlation between adiabatic shear failure and stable slip-line field velocity discontinuities. It was shown in finite element simulations that such velocity discontinuities can be identified by maxima in shear strain rate [43].

Meyer and Pursche [49] provide an up to date and comprehensive account of the material properties that most influence the adiabatic shear failure of high-strength low alloy steels. They also examined in detail the importance of various material properties for the initiation of adiabatic shear failure in quenched and tempered HSLA steels. The most important material property, from both qualitative and quantitative analysis of the adiabatic failure, was found to be dynamic thermal softening behaviour (temperature instability), Figure 18.

Adiabatic shear is a very important failure mechanism for high strength armour steels because it results in low energy failure mechanisms over a range of hardness values where reduced ballistic performance is normally found. While much work has been conducted in

the past, adiabatic shear will continue to be an important research topic for many years to come.

No.	Property	Qualitative Consideration	Quantitative Consideration	Assessment Rating
		Threshold Value	R^2 -Value	
1	Temperature instability from dynamic stress–temperature behaviour	Yes	0.95	Very good
2	Shear failure from dynamic hat-shaped test	Yes	0.95	
3	Stress instability from dynamic stress–temperature behaviour	Yes	0.94	
4	Area under the dynamic stress–temperature curve	Yes	0.94	
5	Hardness	Yes	0.91	Good
6	Failure energy, according to Grady	Yes	0.87	
7	Dynamic compression flow stress at room temperature	Yes	0.86	
8	Dynamic tensile strength at room temperature	Yes	0.84	
9	Decline behaviour from dynamic compression-stress–temperature behaviour	Yes	0.79	
10	Decline behaviour from dynamic stress–compression behaviour of compression/shear test	Yes	0.61	Insufficient
11	Uniform elongation under dynamic loading	Yes	0.47	
12	Simplified Culver equation	Yes	0.02	–

Figure 18: A ranking of material properties in accordance with their propensity to fail by adiabatic shear (from [49]).

7. Structural Cracking

An armoured structure is considered to fail when cracking occurs either rapidly or propagates through an armour plate such that the local structure is unable to support any additional structural or impact loads. The avoidance of cracking, termed structural cracking, is paramount to structural integrity and the maintenance of the ballistic integrity of armour steels. Appropriate armour steel selection and fabrication will avoid, or at least

minimise the initiation or growth of structural cracking, and thus expensive structural remedial repairs.

Structural cracking in armour steels results from the precise metallurgical details produced by fabrication and as such cannot be predicted numerically with any fidelity. Tiny cracks, often less than a millimetre, are below a practical size for crack detection and are all that is required for free crack propagation but it is important to understand that these cracks are usually not caused by, or necessarily propagated by, fatigue. Tensile residual stresses play a dominant role in structural cracking as they can be as high as the yield stress, which is considerable for many armour steels. The dynamic loads from vehicle operation are very small by comparison [50]!

7.A. Cracking associated with Welding

A range of defects, including cracks can be caused by welding processes, examples of which are shown in Figure 19, many of which can lead to structural cracking problems. The avoidance of weld defects, particularly cracking, is the reason why armour steel welding processes are carefully controlled through various welding standards, and have allowed rolled homogenous armour [10], a much higher strength steel than normal quenched and tempered steels, to be successfully welded into a range of armoured vehicle structures over many decades.

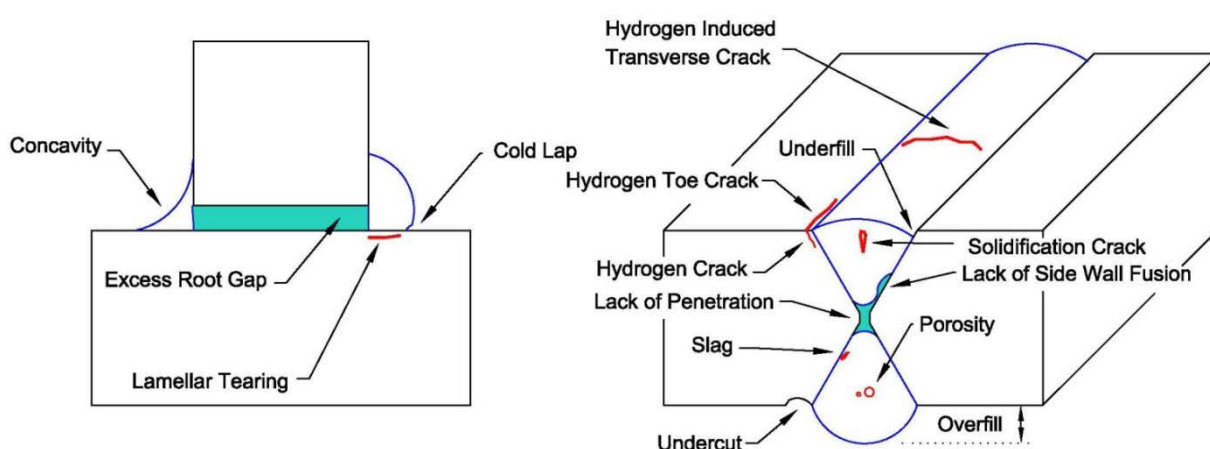


Figure 19: Schematic of weld defects and discontinuities [51]. Cracks are depicted in red and gaps between materials are depicted in green.

However, much harder armour steels are now also required to be welded. While high hardness armour [11] was originally developed as a non-structural armour, it is now also used as a welded structural armour, e.g. for wheeled light armoured vehicles. Such steels must be carefully selected and specific fabrication procedures need to be followed to minimise the real risks of structural cracking.

Hydrogen induced cold cracking, most common in the Heat Affected Zone (HAZ) of armour steels where it is sometimes known as weld-toe or underbead cracking, is a significant risk when welding quenched and tempered steels and can result in the

appearance of cracks sometimes long after welding has been completed. A number of welding procedures have been developed to avoid cracking in both rolled homogenous armour [52] and high hardness armour [53] steels. Cracking can also be found after repair welding. The repair of welded armour steel can be particularly difficult due to the high level of constraint in some weldments and the presence of high residual stresses.

7.B. Fatigue Cracking

While fatigue cracking is possible in armour steels, in practical terms it is rare as armoured structures by definition are normally overdesigned from a fatigue point of view. When found, fatigue is normally associated with poor weld joint design resulting in complex residual stresses with dynamic loads that are either unforeseen non-design loads or occur over an extended period beyond a sensible service life.

7.C. Stress Corrosion Cracking

Stress corrosion (and corrosion fatigue when dynamic loading is significant) is an environmentally assisted form of cracking. For instance, high strength armour steels have been shown to be much more susceptible to cracking in saltwater than when exposed to other environments, even tropical environments [54]. Stress corrosion cracking occurs, following crack initiation, when all three of the following conditions are present:

- i. An applied or residual stress
- ii. A susceptible microstructure
- iii. A corrosive environment

If any one of these three conditions is removed, then stress corrosion cracking will be prevented. As high strength armour steels will have a susceptible microstructure, it is important to maintain protective coatings and use procedures that minimise the build-up of residual stresses during fabrication.

7.D. Delayed Cracking

‘Delayed cracking’ can be a serious structural issue. Such cracking is known to occur either during, or after, completion of the fabrication of an armoured vehicle and can be quite widespread. Cracks with a length measured in decimetres rather than millimetres can be discovered long after fabrication has been completed, but are not considered to extend by fatigue, though stress corrosion can sometimes play a role. Figure 20, shows a typical structural crack caused by delayed cracking.



Figure 20: Structural crack in high hardness armour caused by delayed cracking (after [55]). This crack is over 200 mm in length.

Sometimes armour plates even crack prior to welding, with such cracking sometimes occurring around the periphery of a free-standing plate. Even after fabrication, delayed cracking is often found to originate from free plate edges. The five main causes of delayed cracking are:

- 1) A susceptible microstructure of sufficient hardness that allows cracks of a critical length to freely propagate;
- 2) A tensile residual stress field;
- 3) Presence of hydrogen within the microstructure, leading to hydrogen-induced cold cracking in the plate Heat Affected Zones (HAZ) adjacent to welds [52,53];
- 4) Insufficiently controlled material specifications leading to microstructures with reduced toughness and greater susceptibility to crack propagation [56]; and
- 5) Crack starters associated with the presence of untempered martensite on the free edges of armour plates after cutting [56]. Cracks of a critical length can form and thus propagate into the rest of the plate.

Delayed cracking is prevented or reduced by:

- 1) Adopting low hydrogen welding procedures;
- 2) Specifying an armour steel with tight compositional limits and high toughness requirements; and
- 3) Using armour plate cutting methods that reduce the size of untempered martensite at the free edges of plates, e.g. laser cutting or even water-jet cutting to eliminate untempered martensite entirely.

8. Speciality Armour Steels

8.A. Dual Hardness and Maraging Steels

Very high hardness armour is required to shatter armour piercing projectiles [1]. Homogenous armour of such hardness would normally be brittle and prone to shatter. This led to the concept of dual hardness armour steels, where a hard front face defeats a

projectile by breaking it and the more ductile rear layer prevents penetration by the residual projectile, arrests any cracks and also maintains the structural integrity of the laminate [1].

A great deal of development work in the 1960s led to the specification of roll-bonded dual hard plate in MIL-A-46099C [17] which had a front layer hardness of 601-712 HB with a rear layer hardness of 461-534 HB. These materials are both Ni-Mo-Cr steels with a higher carbon content in the front layer to achieve the required hardness [57]. A strong metallurgical bond between the layers is required for high ballistic resistance [1] and for good multi-hit capability, which is achieved by hot rolling. However, the ballistic performance of such materials can be problematic unless a strong metallurgical bond can be produced reliably.

Electroslag remelting (ESR) (refer Section 8.2) was used to produce dual hardness armour with front and rear face hardnesses (500-560HB front, 340-370HB rear) better optimised for improved fragmentation protection [57]. In this case, a reliable metallurgical bond between the two steel layers was achieved as the ESR process welds one of the layers (which is molten) to the other, which is in a solid or partially molten state [57]. While this steel was not fully optimised for projectile protection, Figure 21 shows the increase in ballistic performance that can be achieved over both RHA and HHA [57].

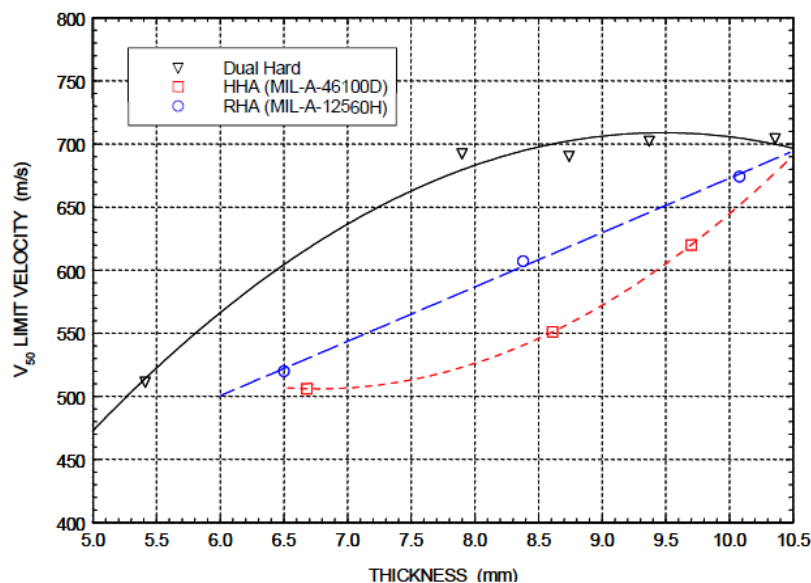


Figure 21: The V_{50} ballistic limit for Bulgarian dual hardness armour, HHA and RHA against 0.30 Cal APM2 at 0° obliquity (after [57]).

Explosive bonding is also used commercially to produce dual hardness (60HR_c/50HR_c) armour plate, where two Ni-Mo-Cr armour steel layers are bonded explosively together to form a strong metallurgical and mechanical bond. The explosive bonding process produces a stronger metallurgical bond than roll bonding. This is because explosive bonding [58] cleans metal oxides from the two bonding surfaces immediately before they are bonded and produces a wavy interface between the two bonding layers, which also has a finer grain size. This and the mechanical interlock between the two wavy layers

maximises the shear strength of the interface between the layers so that it better withstands shear from bending deformations, better maintaining the integrity of the laminate, particularly when it is impacted multiple times. Figure 22 shows an example of the mechanical interlock that can be achieved between a quenched and tempered martensitic steel and a soft austenitic steel.



Figure 22: Microstructure of explosively-welded steels demonstrating the wavy mechanical interlock between a 440HV martensitic steel (darker microstructure) and a 215HV austenitic steel (white, unetched microstructure). Note the shear bands in the quenched and tempered martensitic steel. Scale bar is 200 μm (from [59]).

An important advantage of some Ni-Mo-Cr dual hardness armour steels is that they can be softened by a solution annealing heat treatment to allow easy fabrication (forming, cutting, drilling, welding, etc.). Such steels are then easily re-hardened by a lower aging heat treatment, followed by air-cooling to the final design hardnesses. This offers considerable flexibility for fabrication. While such steels will be more expensive than conventional quenched and tempered steels, they offer the ability to form large structures or complex shapes prior to any final hardening heat treatment.

Homogenous Ni-Cr-Mo steels are available that meet Class 2 MIL-DTL-46100E [11]. These steels include additional Ni, Cr and Mo compared to conventional quenched and tempered HHA to increase hardenability and toughness and allow an aging heat treatment, followed by air cooling [60]. Such steels are a logical development from the Ni-Mo-Cr maraging dual hardness steel compositions discussed above and allow easier fabrication, including forming, cutting and drilling as well as any post fabrication heat treatments to recover ballistic properties. The slower air cooling also results in higher dimensional stability.

8.B. ESR Steels

Electroslag Refining (or Remelting) (ESR) has been used to produce cleaner steels with more uniform composition than conventional high quality steels. Sulphur and non-metallic inclusions (and their size) are significantly reduced by this process. ESR steels therefore have better ductility and toughness, particularly in the through-thickness direction, than equivalent conventional steels that are more anisotropic [32].

Figure 23 shows how ESR processed-steels (Coupons B and C) can achieve much greater through-thickness (short transverse) toughness than the same steel which has been just vacuum arc remelted (Coupon A), even though these steels have similar toughness in the plane of the plate. This correlates to observations that ESR steels show improved spallation resistance against through-thickness stress waves arising from contact detonations of explosives [61].

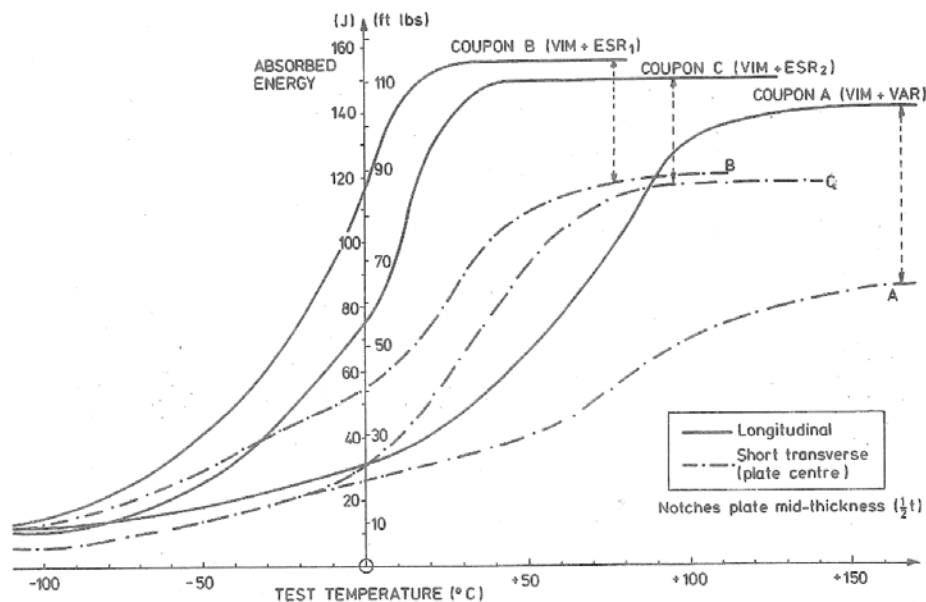


Figure 23: Longitudinal and short transverse Charpy curves for Vacuum Induction Melted (VIM) steel that is followed by either ESR (Coupons B and C) or Vacuum Arc Remelting (VAR) (Coupon A) (from [61]).

ESR steels have improved ballistic resistance over a hardness range where adiabatic shear occurs [62] and thus are best suited for applications that require such steel hardnesses. Any enhancement of ballistic resistance against small arms projectiles would be due to the greater work of plug tear out once asymmetric deformation occurs [14]. The overall move by steel makers to continuous casting and cleaner steel making processes as well as the cost of the ESR process and its complexity has meant that it has not been widely applied for armour applications in the western world.

9. Armour Steel Specifications and Standards

In practical terms, armour is required to deliver optimized performance against a range of battlefield threats, including armour piercing and fragmentation threats. Such protection has to be provided at realistic areal densities for an affordable price. Defence specifications are used to define the optimum use and control the quality assurance of the ballistic and mechanical properties for particular applications. As rolled armour steel has continued to be the predominant armour material for many ballistic applications, this section is concerned with wrought rather than cast steel armour.

Two of the most common armour steel grades in use are MIL-DTL-12560K Class 1 Rolled Homogenous Armor (RHA) with a hardness range of 250-410HB [10] and MIL-DTL-46100E High Hardness Armor (HHA) with a hardness range of 477-534HB [11]. Both of these specifications had their origins in World War II and have not changed markedly since [8], though the former was modified after many years to incorporate a new class of wrought armour plate, Class 4, which is heat treatable to higher hardness ranges than Class 1 as well as other improvements. MIL-DTL-32332 [12] is a new specification that specifies ultra-high hardness steels with hardnesses in excess of 570HB.

There has been development and application of unified armour steel specifications that control armour steel properties over a wide range of steel hardness. Australian DEF(AUST) 8030 [35] and UK DEF STAN 95-24 [63] are examples of such unified specifications, Tables I and II comparing these specifications with the U.S. Military Specifications. DEF(AUST) 8030 controls mechanical and chemical properties over a full range of functional rolled homogenous armour steel classes. It is a performance-based specification, allowing a designer the freedom to choose an armour steel that best meets their needs while defining ballistic performance quality assurance requirements and, importantly, ensuring that the structural integrity of the resulting armoured structure will also meet a minimum standard [64].

Increasing armour steel hardness will usually reduce the toughness of steels. Hardness limits, Table I, are therefore set for specific steel armour classes to control toughness during production, Table II, and reduce the risk of shattering or other brittle failures for specific steel compositions and applications. For example, HHA is highly susceptible to stress-corrosion cracking in marine (saltwater) environments.

Table I: Hardness of Armour Steel Grades less than 35 mm (after [35]).

Armour Class According to DEF(AUST) 8030	Hardness Equivalences (HB)		
	DEF(AUST) 8030 ¹	U.S. Specification Approx. Nominal Equivalent Grade	DEF STAN 95-24 Approx. Nominal Equivalent Grade
Class 1	Not Explicitly Specified	No Equivalent	No Equivalent
Class 2	260-310	MIL-DTL-12560K: Class 2 ≤50.8 mm 260-310	Class 1 262-311
Class 3	340-390	MIL-DTL-12560K: Class 1 6.35 to ≤15.8 mm: 340-390 15.9 to <28.6 mm: 330-380 28.6 to ≤50.8 mm: 310-360	Class 2 <9 mm: ≥341 9 to <15 mm: ≥311 15 to <35 mm: ≥285
Class 4	370-430	MIL-DTL-12560K: Class 1 ≤6.3 mm: 360-410	No Equivalent
Class 5	420-470	MIL-DTL-12560K: Class 4 ≤69.9 mm: 420-470	Class 3A 5 to <50 mm: 420-480
Class 6	477-534	MIL-DTL-46100E <50.8 mm: 477-534	Class 3 <15 mm: 470-540 15 to <35 mm: 470-535
Class 7	≥570	MIL-DTL-32332: Class 1 <16 mm: ≥570	Class 5 560-655
Class 8	≥570	MIL-DTL-32332: Class 2 <16 mm: ≥570	No Equivalent

¹Each hardness range in DEF(AUST) 8030 applies for all thicknesses from 3-35 mm, unless otherwise specified.

While ballistic performance will generally increase with hardness, this will depend on the threat projectile and armour thickness and toughness. It is also the case that the optimum armour choice will depend on whether the armour is to be applied as a stand-alone structural armour or applique armour. The armour designers are to ensure that they have selected the armour class that offers the best combination of ballistic performance and structural properties appropriate for the intended application, i.e. Table III. It is respondent on the armour designer to choose the grade and thus armour properties (strength/hardness/toughness) that both maximise protection and minimise through-life costs for any specific armour application.

Table II: Charpy Toughness of Armour Steels less than 35 mm. Charpy Toughness measured at -40 °C according to AS 1544.2 (DEF(AUST) 8030) or BS EN 10045-1 (DEF(AUST) 8030 and DEF STAN 95-24) or ASTM E23 and ASTM A370 (U.S. specifications) (after [35]).

Armour Class According to DEF(AUST) 8030	Minimum Charpy Toughness (J)		
	DEF(AUST) 8030	U.S. Specification Approx. Nominal Equivalent Grade	DEF STAN 95-24 Approx. Nominal Equivalent Grade
Class 1	Not Explicitly Specified	No Equivalent	No Equivalent
Class 2 260-310HB	40	MIL-DTL-12560K: Class 2 260-270HB: 75.9 270-280HB: 69.1 280-290HB: 62.4 290-300HB: 55.6 300-310HB: 48.8	Class 1 260-310HB: 40
Class 3 340-390HB	20	MIL-DTL-12560K: Class 1 340-350HB: 29.8 350-360HB: 25.7 360-370HB: 24.4 370-380HB: 23.0 380-470HB: 21.7	Class 2 <9 mm: ≥341HB: 20 9 to <15 mm: ≥311HB: 20 15 to <35 mm: ≥285HB: 25 35 to <50 mm: ≥262HB: 30
Class 4 370-430HB	18	MIL-DTL-12560K: Class 1 370-380HB: 23.0 380-470HB: 21.7	No Equivalent
Class 5 420-470HB	16	MIL-DTL-12560K: Class 4 420-470HB: 21.7	Class 3A 5 to <50 mm: 420-480HB: 16
Class 6 477-534HB	16	MIL-DTL-46100E 477-534HB: 16.3	Class 3 <15 mm: 470-540HB: 16 15 to <35 mm: 470-535HB: 29
Class 7 ≥570HB	12	MIL-DTL-32332: Class 1 ≥570HB: 8.1	Class 5 560-655HB: 5
Class 8 ≥570HB	8.1	MIL-DTL-32332: Class 2 ≥570HB: 8.1	No Equivalent

Table III: Intended use for each armour class in DEF(AUST)8030 (after [35]).

Armour Class According to DEF(AUST) 8030	DEF(AUST) 8030	
	DEF(AUST) 8030 Hardness	Intended Use for each Armour Class
Class 1	Not Explicitly Specified	<p>Class 1 armour grade allows the application of structural grades of quenched and tempered steels for specialised armour applications, for example, naval applications. Class 1 armour has excellent toughness and good weldability and formability.</p> <p>Steels nominated as Class 1 armour shall meet the requirements of a nominated structural steel specification. AS 3597, ASTM A514 or MIL-S-24645A are examples of typical structural steel specifications that would meet the requirements of this class of armour, i.e. they have a minimum 0.2% proof stress of 550 MPa and also meet the additional requirements of Sections 3.4 to 3.9 of this Specification. Class 1 armour is not equivalent to Class 1 armour in MIL-A-12560K.</p>
Class 2	260-310	Class 2 armour is intended for use in those areas where maximum resistance to failure under conditions of blast loading and fragmentation protection is required and where resistance to penetration by armour-piercing ammunition is of secondary importance to resistance. Class 2 armour is intended for use for protection against landmines and other blast-producing weapons. Class 2 armour can be cold worked and is weldable.
Class 3	340-390	Class 3 armour is intended for use in applications where very good resistance to penetration is combined with excellent structural properties. Class 3 armour can be cold worked and is weldable.
Class 4	370-430	Class 4 armour is heat treated to higher hardness levels than Class 3 armour to further increase resistance to penetration whilst maintaining similar structural properties to Class 3 armour. Class 4 armour can offer an advantage over Class 3 and Class 5 armour for certain applications.
Class 5	420-480	Class 5 armour is heat treated to higher hardness levels than Class 4 armour to further increase resistance to penetration. Class 5 armour is intended as a tougher alternative for Class 6 armour and can ballistically outperform it.

Class 6	477-534	Class 6 armour was originally created for applique armour only and can be used with care for welded structural applications.
Class 7	≥ 570	Class 7 armour is intended for use as a non-structural stand-alone or applique armour that is designed for better resistance to penetration than Class 6 armour.
Class 8	≥ 570	Class 8 armour is intended for use as a non-structural stand-alone or applique armour that is designed for better resistance to penetration than Class 7 armour.

10. Conclusions

The relationship between armour steel mechanical properties, specifically their mechanical metallurgy, and ballistic performance has been discussed, where such performance is primarily determined by material strength, hardness and high strain rate behaviour. Other important topics such as toughness, the adiabatic shear phenomenon; structural cracking; and dual hardness and electrosag remelted armour steels are also discussed along with armour steel specifications and standards. It is considered that armour steels will not only continue to improve but will also continue to dominate vehicle armour designs well into the future.

11. References

1. S.J. Manganello and K.H. Abbott, Metallurgical Factors Affecting the Ballistic Behaviour of Steel Targets, J. Mat., Vol. 7, 1972, pp. 231-239.
2. G.I. Taylor, The Formation and Enlargement of a Circular Hole in a Thin Plastic Sheet, Quart J. Mech. and Appl. Math., Vol. 1, 1948, pp. 103-124.
3. R.L. Woodward, The Penetration of Metal Targets by Conical Projectiles, Int. J. Mech. Sci., Vol. 20, 1978, pp. 349-359.
4. D. Tabor, The Hardness of Metals, Clarendon Press, Oxford, 1951, p. 108.
5. R.L. Woodward, Materials for Projectile Disruption, Materials Forum, Vol. 12, 1988, pp. 26-30.
6. D. Tabor, The Hardness of Metals, Clarendon Press, Oxford, 1951, p. 105.
7. Ibid, p. 112.
8. W.A. Gooch, D.D. Showalter, M.S. Burkins, V. Thorn, S.J. Cimpoeru and R. Barnett, Ballistic Testing of Australian Bisalloy Steel for Armor Applications, 23rd Int. Symposium on Ballistics, Tarragona, Spain, 16-20 April 2007, Vol. 2, 2007, pp. 1181-1188.
9. S. Ryan, H. Li, M. Edgerton, D. Gallardy, and S.J. Cimpoeru, The Ballistic Performance of an Ultra-High Hardness Armour Steel: An Experimental Investigation, Int. J. of Impact Engng, Vol. 94, 2016, pp. 60-73.

10. U.S. Detail Specification, MIL-DTL-12560K(MR), Armor Plate, Steel, Wrought, Homogeneous (For use in Combat-Vehicles and for Ammunition Testing), 7 Dec. 2013.
11. U.S. Detail Specification, MIL-DTL-46100E(MR), Armor Plate, Steel, Wrought, High Hardness, 9 July 2008.
12. U.S. Detail Specification, MIL-DTL-32332(MR), Armor Plate, Steel, Wrought, Ultra-High Hardness, 24 July 2009.
13. E. Rapacki, K. Frank, B. Leavy, M. Keele, and J. Prifti, Armor Steel Hardness Influence on Kinetic Energy Penetration, 15th Int. Symposium on Ballistics, Jerusalem, Israel, 21-24 May 1995, Vol. 1, 1995, pp. 323-330.
14. R.L. Woodward, The Interrelation of Failure Modes Observed in the Penetration of Metallic Targets, Int. J. Impact Engng, Vol. 2, 1984, pp. 121-129.
15. W.A. Gooch, M.S. Burkins, R. Squillacioti, R. Stockman Koch, H. Oscarsson, and C. Nash, Ballistic Testing of Swedish Steel for U.S. Armor Applications, 21st Int. Symposium on Ballistics, Adelaide, Australia, 19-23 April 2004, Vol. 1, 2004, pp. 174-181.
16. D.D. Showalter, W.A. Gooch, M.S. Burkins and R.S. Koch, Ballistic Testing of SSAB Ultra-High hardness Steel for Armor Applications, 24th Int. Symposium on Ballistics, New Orleans, LA, 22-26 September 2008, Vol. 1, 2008, pp. 634-642.
17. U.S. Military Specification, MIL-A-46099C, Armor Plate, Steel, Roll-Bonded, Dual Hardness (0.187 Inches to 0.700 Inches Inclusive), 14 September 1987.
18. T. Borvik, S. Dey and A.H. Clausen, Perforation Resistance of five different High Strength Steel Plates subjected to Small Arms Fire, Int. J. Impact Engng, Vol. 36, 2009, pp. 948-964.
19. R.L. Woodward and S.J. Cimpoeu, unpublished DST Group research.
20. S.J. Cimpoeu, The Flow Stress of a 0.21% C Mild Steel from Strain Rates of 10^{-3} to 2×10^4 sec⁻¹, J. Mat. Sci. Lett., Vol. 9, 1990, pp. 198-199.
21. L.W. Meyer, T. Halle, N. Herzig, L. Krüger and S.V. Razorenov, Experimental Investigations and Modelling of Strain Rate and Temperature Effects on the Flow Behaviour of 1045 Steel, J. Phys IV France, Vol. 134, 2006, pp. 75-80.
22. H. Nahme and N. Lach, Dynamic Behavior of High Strength Armor Steels, J. Phys IV France, Vol. 7, 1997, C-373 - C377.
23. V. Schulze and O. Vöhringer, Influence of Alloying Elements on the Strain Rate and Temperature Dependence of the Flow Stress of Steels, Metallurgical and Materials Transactions A (Physical Metallurgy and Materials Science), Vol. 31A, 2000, pp. 825-830.
24. G.R. Johnston and W.H. Cook, A Constitutive Model and Data for Metals subjected to Large Strains, 7th Int. Symp. on Ballistics, The Hague, Netherlands, 1983, pp. 541-547.
25. F.J. Zerilli and R.W. Armstrong, J. Appl. Physics, Vol. 61, 1987, pp. 1816-1825.
26. W.A. Spitzig, R.J. Sober, and O. Richmond, Pressure Dependence of Yielding and Associated Volume Expansion for Tempered Martensite, Acta Metall., Vol. 23, 1975, pp. 885-893.
27. L.W. Meyer and S. Abdel-Malek, Strain rate dependence of strength-differential effect in two steels, Le Journal de Physique IV 10, PR9, 2000, Pr9-63-Pr9-68.
28. T. Weerasooriya and P. Moy, Effect of Strain Rate on the Deformation of Behavior of Rolled-Homogenous Armor (RHA) Steel at Different Hardnesses, 2004 SEM Congress and Exposition on Experimental Mechanics, CostaMesa, CA, 2004.

29. R.L. Woodward and N.J. Baldwin, Oblique Perforation of Steel Targets by .30 Cal. AP M2 Projectiles, *Int. J. Mech. Engng Sci.*, Vol. 21, 1979, pp. 85-91.
30. G.E. Dieter, *Mechanical Metallurgy*, 2nd Edn, McGraw-Hill, 1981.
31. P.W. Leach and R.L. Woodward, The Influence of Microstructural Anisotropy on the Mode of Plate Failure during Projectile Impact, *J. Mat. Sci.*, Vol. 20, 1985, pp. 854-858.
32. A.C. Mackenzie, J.W. Hancock and D.K. Brown, On the Influence of State of Stress on Ductile Failure Initiation in High Strength Steels, *Eng. Fract. Mech.*, Vol. 9, 1977, pp. 168-188.
33. K. Sato, Q. Yu, J. Hiramato, T. Urabe, A. Yoshitake, A method to investigate strain rate effects on necking and fracture behaviours of advanced high-strength steels using digital imaging strain analysis, *Int. J. Impact Engng*, Vol. 75, 2015, pp. 11-26.
34. W.R. Whittington, A.L. Oppedal, S. Turnage, Y. Hammi, H. Rhee, P.G. Allison and M.F. Horstemeyer, Capturing the Effect of Temperature, Strain Rate and Stress State on the Plasticity and Fracture of Rolled Homogenous Armour (RHA) steel, *Mat. Sci. and Engng*, Vol. 594, 2014, pp. 82-88.
35. Australian Defence Standard, DEF(AUST) 8030, Rolled Armour Plate, Steel (3-35 mm).
36. Z. Shah Khan, Unpublished DST Group Research.
37. N. Herzig, N.W. Meyer, F. Pursche and K. Hüsing, Relation between Dynamic Strength and Toughness Properties and the Behavior under Blast Conditions of High Strength Steels, 7th Int. Symp. on Impact Engng, ISIE 2010, Warsaw, Poland, 4-7 July 2010.
38. A.L. Wingrove and G.L. Wulf, Some Aspects of Target and Projectile Properties on Penetration Behaviour, *J. Aust. Inst. Met.*, Vol. 18, 1973, pp. 167-172.
39. C. Zener and J.H. Hollomon, Effect of Strain Rate Upon Plastic Flow of Steel, *J. of Appl. Phys.*, Vol. 15, pp. 22-32.
40. R.L. Woodward, The Penetration of Metal Targets which Fail by Adiabatic Shear Plugging, *Int. J. Mech. Sci.*, Vol. 20, 1978, pp. 599-607.
41. R.F. Recht, Catastrophic Thermoplastic Shear, *J. Appl. Mech.*, Vol. 31E, 1964, pp. 189-193.
42. A.J. Bedford, A.L. Wingrove and K.R.L. Thompson, The Phenomenon of Adiabatic Shear, *J. Aust. Inst. Met.*, Vol. 19, 1974, pp. 61-73.
43. C.J. Flockhart, R.L. Woodward, Y.C. Lam and R.G. O'Donnell, The Use of Velocity Discontinuities to Define Shear Failure Trajectories in Dynamic Plastic Deformation, *Int. J. Impact Engng*, Vol. 11, 1991, pp. 93-106.
44. R. Dornmeier, The adiabatic shear phenomena. Impact loading and dynamic behavior of materials Vol. 1, C.Y. Chiem, H.D. Kunze, and L.W. Meyer, Eds., DGM Informationsgesellschaft, Oberursel, 1988, pp. 43-56.
45. X.B. Wang, Adiabatic shear localization for steels based on Johnson-Cook-Model and second- and fourth-order gradient plasticity models. *Journal of Iron and Steel Research International*, Vol. 14, 2007, pp. 56-61.
46. R.G. O'Donnell and R.L. Woodward, Instability during High Strain Rate Compression of 2024 T351 Aluminium, *J. Mat. Sci.*, Vol. 23, 1988, pp. 3578-3587.
47. S.J. Cimpoeu and R.L. Woodward, High Strain Rate Properties of Three Liquid Phase Sintered Tungsten Alloys, *J. Mat. Sci. Lett*, Vol. 9, 1990, pp. 187-191.
48. M.E. Backman and S.A. Finnegan, The Propagation of Adiabatic Shear, in *Metallurgical Effects at High Strain Rates* (edited by Rohde, Butcher, Holland and Karnes), pp. 531-543. Plenum, New York, 1973.

49. L. W. Meyer and F. Pursche, in *Adiabatic Shear Localization*, Frontiers and Advances, eds B. Dodd and Y. Bai, 2nd Edn, Elsevier, London, 2012, p. 85.
50. S.J. Cimpoeru, The Measurement of Dynamic Structural Stresses in a Light Armoured Vehicle, Fifth Australasian Aeronautical Conference, 13-15 Sept. 1993, Melbourne, IE(Aust.), 1993, pp. 541-547.
51. J. Donato, Unpublished DST Group Research.
52. J.C. Ritter, B.F. Dixon and N.J. Baldwin, Deformation and Weld Repair of Armour Steel, *Materials Forum*, Vol. 13, 1989, p. 216-224.
53. S. J. Alkemade, The weld cracking susceptibility of high hardness armour steel. DSTO Technical Report, DSTO-TR-0320, March 1996.
54. M.Z. Shah Khan, S.J. Alkemade and G.M. Weston, Fracture Studies on High Hardness Bisalloy 500® Steel, DSTO Research Report, DSTO-RR-0130, March 1998.
55. S.J. Alkemade, Unpublished DST Group Research.
56. M.G.H. Wells, R.K. Weiss, J.S. Montgomery and T.G. Melvin, LAV Armor Plate Study, U.S. Army Materials Technology Laboratory Report, MTL TR 92-26, April 1992.
57. W. Gooch, M. Burkins, D. Mackenzie and S. Vodenicharov, Ballistic Analysis of Bulgarian Electroslag Remelted Dual Hard Steel Armor Plate, 22nd Int. Symposium on Ballistics, Vancouver, BC, Canada, 14-18 Nov. 2005, Vol. 2, 2005, pp. 709-716.
58. T.Z. Blazynski, *Explosive Welding, Forming and Compaction*, Springer, 2012.
59. C. Choi, M. Callaghan, P. van der Schaaf, H. Li and B. Dixon, Modification of the Gurney Equation for Explosive Bonding by Slanted Elevation Angle, DSTO Technical Report, DSTO-TR-2960, April 2014.
60. W. Gooch, D. Showalter, M. Burkins, J. Montgomery, R. Squillacioti, A. Nichols, L. Martin, R. Bailey, G. Swiatek, Development and Ballistic Testing of a New Class of Auto-Tempered, High Hard Steels under Military Specification MIL-DTL-46100, TMS 2009, San Francisco, CA, 15-19 February 2009.
61. A. Doig, Comparative Anisotropy of Quenched and Tempered Alloy Steel Plates made by High Quality Air Melting, ESR, VIM&VAR, and VIM&ESR processes, Sixth International Vacuum Metallurgy Conference on Special Melting, San Diego, CA, April 1979.
62. J.D.W. Rawson and D.I. Dawson, British Steel Corporation Corporate Laboratories Report, MG/34/72, 1972.
63. UK Defence Standard, DEF STAN 95-24, Armour Plate, Steel (3-160 mm), Issue 3, 2004.
64. S.J. Cimpoeru and S.J. Alkemade, Guidelines for Effective Armour Material Specifications for Defence Applications, Technological and Research Developments in Welded Defence Equipment Conference, WTIA, 2002.

UNCLASSIFIED

DEFENCE SCIENCE AND TECHNOLOGY GROUP DOCUMENT CONTROL DATA				
			1. DLM/CAVEAT (OF DOCUMENT)	
2. TITLE The Mechanical Metallurgy of Armour Steels		3. SECURITY CLASSIFICATION (FOR UNCLASSIFIED REPORTS THAT ARE LIMITED RELEASE USE (U/L) NEXT TO DOCUMENT CLASSIFICATION) <div style="display: flex; justify-content: space-between;"> Document (U) </div> <div style="display: flex; justify-content: space-between;"> Title (U) </div> <div style="display: flex; justify-content: space-between;"> Abstract (U) </div>		
4. AUTHOR(S) Stephen Cimpoeu		5. CORPORATE AUTHOR Defence Science and Technology Group 506 Lorimer Street Fishermans Bend VIC 3207		
6a. DST Group NUMBER DST-Group-TR-3305	6b. AR NUMBER 016-722	6c. TYPE OF REPORT Technical Report	7. DOCUMENT DATE October 2016	
8. Objective ID AV14567385	9. TASK NUMBER ARM07/132	10. TASK SPONSOR AHQ		
13. DOWNGRADING/DELIMITING INSTRUCTIONS		14. RELEASE AUTHORITY Chief, Land Division		
15. SECONDARY RELEASE STATEMENT OF THIS DOCUMENT <div style="text-align: center;"><i>Approved for public release</i></div>				
OVERSEAS ENQUIRIES OUTSIDE STATED LIMITATIONS SHOULD BE REFERRED THROUGH DOCUMENT EXCHANGE, PO BOX 1500, EDINBURGH, SA 5111				
16. DELIBERATE ANNOUNCEMENT No limitations				
17. CITATION IN OTHER DOCUMENTS Yes				
18. RESEARCH LIBRARY THESAURUS armour steels, mechanical metallurgy, high strain rate, adiabatic shear				
19. ABSTRACT Armour steels have historically delivered optimised ballistic performance against a range of battlefield threats and continue to be highly competitive armour materials. The relationship between armour steel mechanical properties, specifically their mechanical metallurgy, and ballistic performance is explained, where such performance is primarily determined by material strength, hardness and high strain rate behaviour. Other important topics such as toughness; the adiabatic shear phenomenon; structural cracking; and dual hardness and electroslag remelted armour steels are also discussed along with armour steel specifications and standards.				

UNCLASSIFIED